Dynamic Analysis and Balancing of an Aircraft Gas Turbine

By

E. J. Gunter, Jr.
Fellow ASME
RODYN Vibration Analysis, Inc.
Charlottesville, Virginia

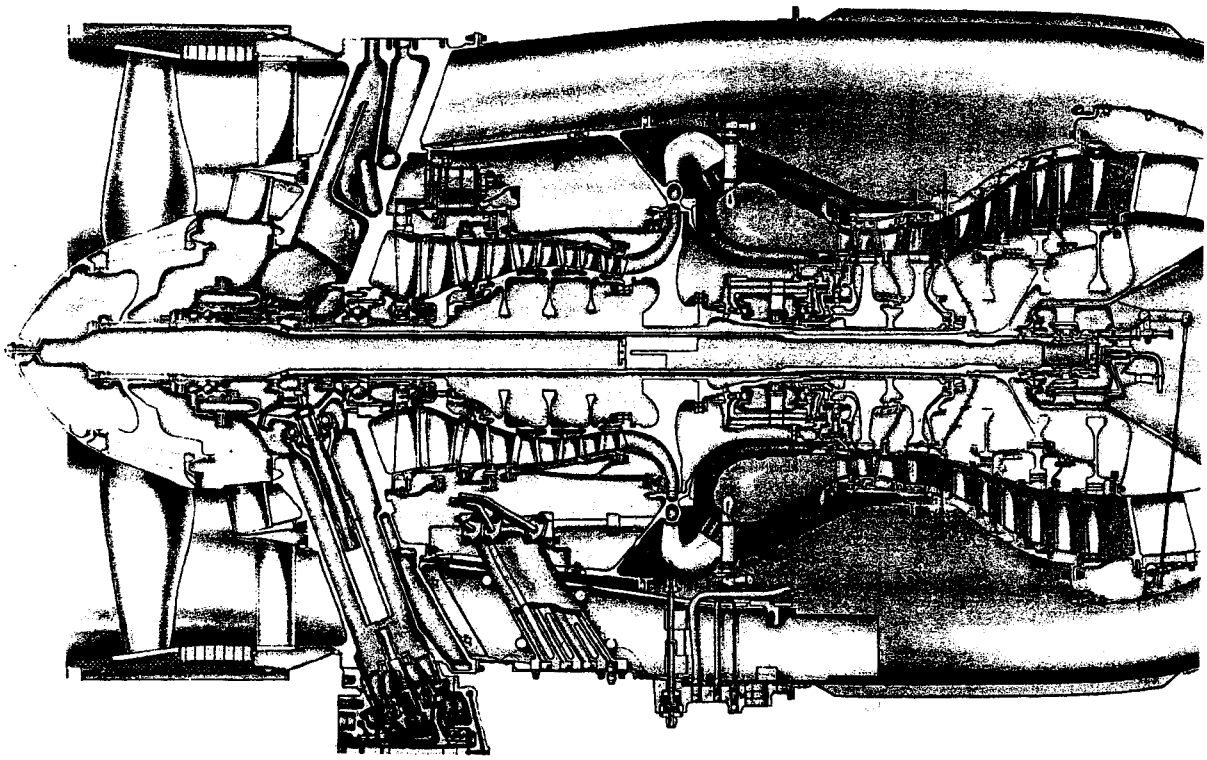

July 2001

Dynamic Analysis and Balancing of an Aircraft Gas Turbine

by

E. J. Gunter, Ph.D.
Fellow ASME

1. Introduction and Engine Vibration Characteristics

Figure 1 represents a photograph of a medium-sized business jet in which the engines are rear-mounted to the fuselage. For the small business-sized jet aircraft, the rear mounting of the engines leads to a more aerodynamically efficient design with a higher cruise range.

Figure 2 represents a schematic drawing of the engine and casing. Indicated on the schematic are the various locations for instrumentation to monitor engine vibrations. These instruments are accelerometers in which the acceleration signal is integrated to determine velocity. There are no displacement probes to directly monitor the shaft motions of either the low pressure or high pressure turbines.

Since these jets have rear-mounted engines, excessive engine vibrations may be transmitted to the fuselage. The fuselage, in turn, may have its own acoustic modes which, under certain circumstances, may be excited by engine response. While the integrity of the engine has never been an issue, there have been occasions when an engine had to be removed for re-balancing due to excessive sound pressure levels generated in the cabin. On larger classes of business aircraft, the apparent passenger noise problem is avoided by having the gallery area next to the engine mounts. However, in the smaller business jets, the executive seating is often in proximity to the engine mounts. When the plane reaches cruising altitude, the accompanying sound pressure level may interfere with normal conversation. Excessive noise levels in the past have led to downtime caused by engine replacement and even loss of sales.

Extensive instrumentation was placed on the engine to determine vibration characteristics in the test cell and also several aircraft were instrumented so that vibration levels could be determined during flight at various altitudes and power levels.

Instrumentation was placed at various locations along the engine casing. Figure 3 represents a comparison of the experimental vibration data obtained at the vertical rear support (RSV), as compared to the original theoretical analysis performed by the engine manufacturer. In the original theoretical analysis, the LP rotor modes were considered well damped and that no rotor modes were predicted to be excited above 3,000 RPM. In the observed experimental data, there are a number of very strong resonant peaks observed at 3,500 RPM, 6,500 RPM, and 7,800 RPM. The nature of these vibrations varies considerably from engine to engine.

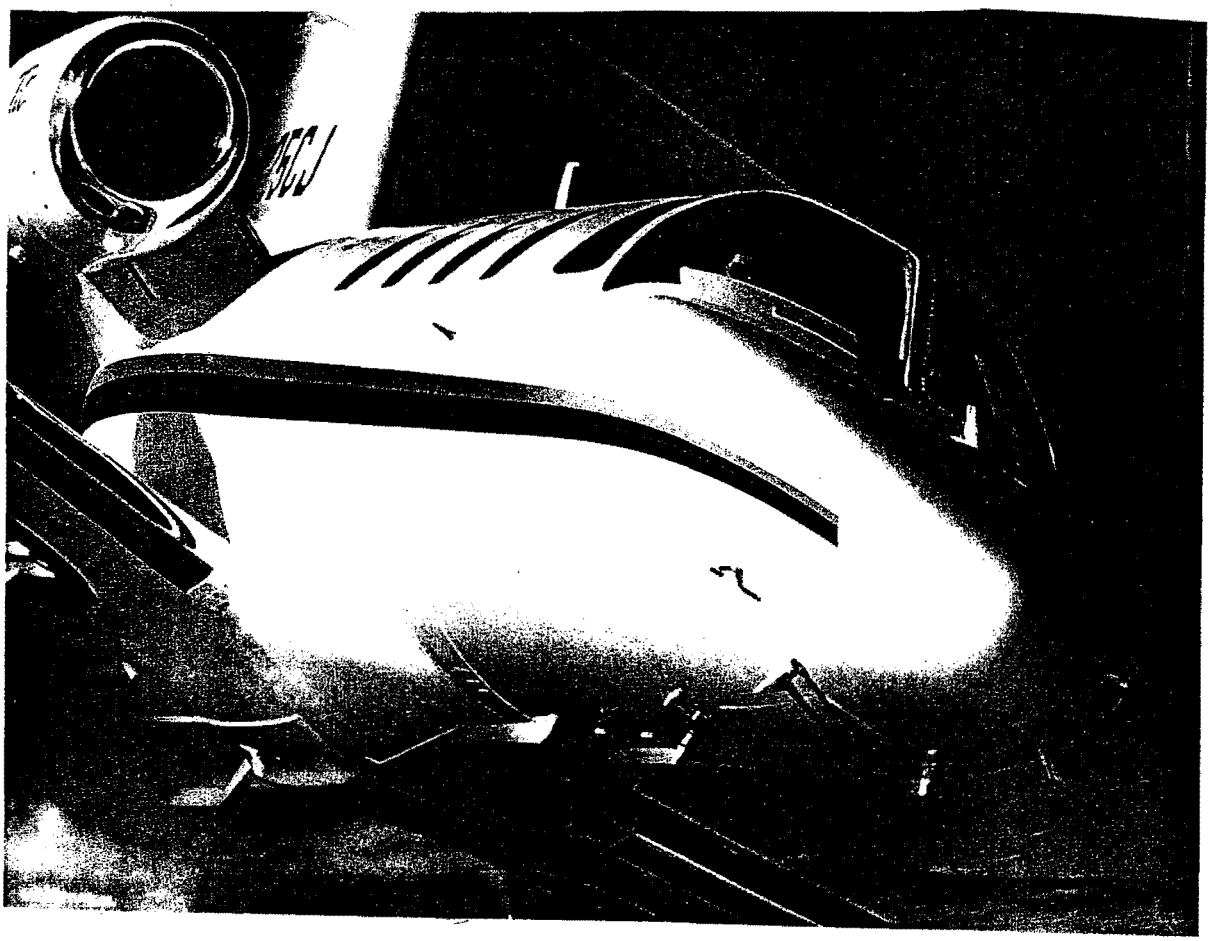

Figure 1. View of Aircraft and Engine

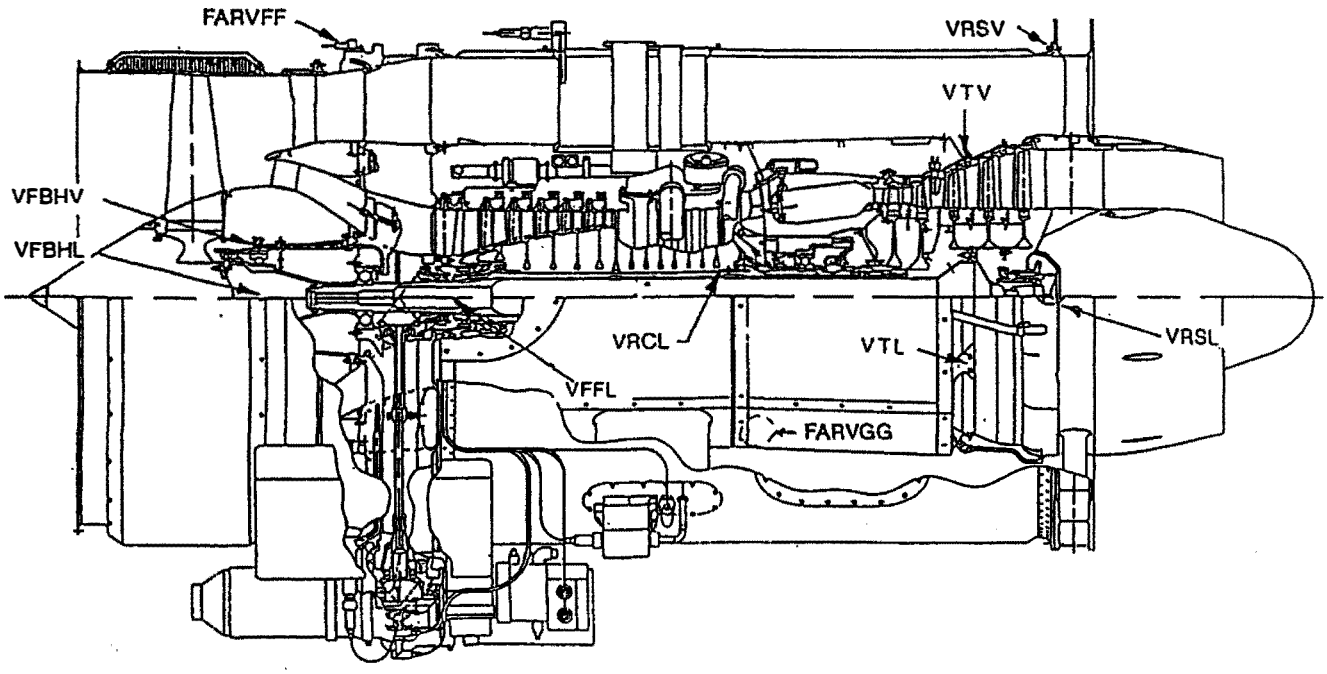

Figure 2. Cross Section of Engine

After several years of investigation, it was determined that the peaks observed are the LP second mode with a locked damper, and the other two modes are the LP third mode interacting with the casing. The sharp resonant peak observed at the LP second mode could be caused by a locked-up damper. The irregular motion observed with the LP third mode above 6,500 RPM may be caused by dead band whirl in the damper clearance space with an inadequate oil supply.

In order to determine more detailed characteristics of the engine vibrational behavior, an experimental engine was instrumented and vibration data was obtained for various values of unbalance placed upon the LP fan rotor. Figure 4 represents the vibration at the far front frame (FARVFF) accelerometer for unbalances ranging from 8.8 to 17.6 grams. Resonant frequencies at 4,000 RPM, 5,000 RPM, and 7,000 RPM are clearly discernable from the data. The resonant frequency at 7,000 RPM is of major concern, as this falls in the operating speed range of the aircraft. The experimental data also shows that the engine may be well balanced by the 8.8 grams placed at 240 degrees.

Single-plane balancing at the test facility proved to be straightforward because of the ability to obtain a timing or key phaser signal from the LP rotor. This, however, is not the case when the aircraft is on the tarmac. Single-plane balancing of the fan rotor while the aircraft is on the runway has been accomplished by means of a laser beam to obtain a timing mark. However, this method is not always successful, particularly in hot, humid conditions where inlet fogging can occur. Under these circumstances, a reliable phase reading cannot be obtained. Based on extensive test cell data, it was determined that a modified form of the three-trial-weight method could be used to greatly speed up the process of trim balancing an engine on the runway. For each day of delay of aircraft delivery, there can be a $10,000 surcharge applied. Therefore, it is essential to have a rapid and reliable method of engine field trim balancing to reduce vibration and sound pressure level measurements in the cabin.

Figure 5a represents the vibration from the accelerometer at the external casing on the rear (VSRV) and on the internal turbine casing (VTV). The internal casing, VTV, shows a response similar to the front frame, with 17.6 grams. The peak response is about 6,700 RPM. However, the response on the rear frame indicates the presence of another mode which increases up to three inches per second. The unbalance in the fan causes a violent excitation of the rear casing. The strong mode seen at the rear is not felt at the front frame. It is therefore apparent that there is a strong rotor-casing interaction in the operating speed range of 6,500 RPM to 7,800 RPM. It was later observed that these engine modes interact with the acoustic cabin modes.

Figure 5b represents the vibration level and phase angle at the internal casing only, VTV. The location of the VTC transducer is on the inner casing and in the plane of rear turbine bearing support. Therefore, the VTV response is an excellent indicator of the LP 2nd mode at 3,600 RPM and the third mode at 6,700 RPM.

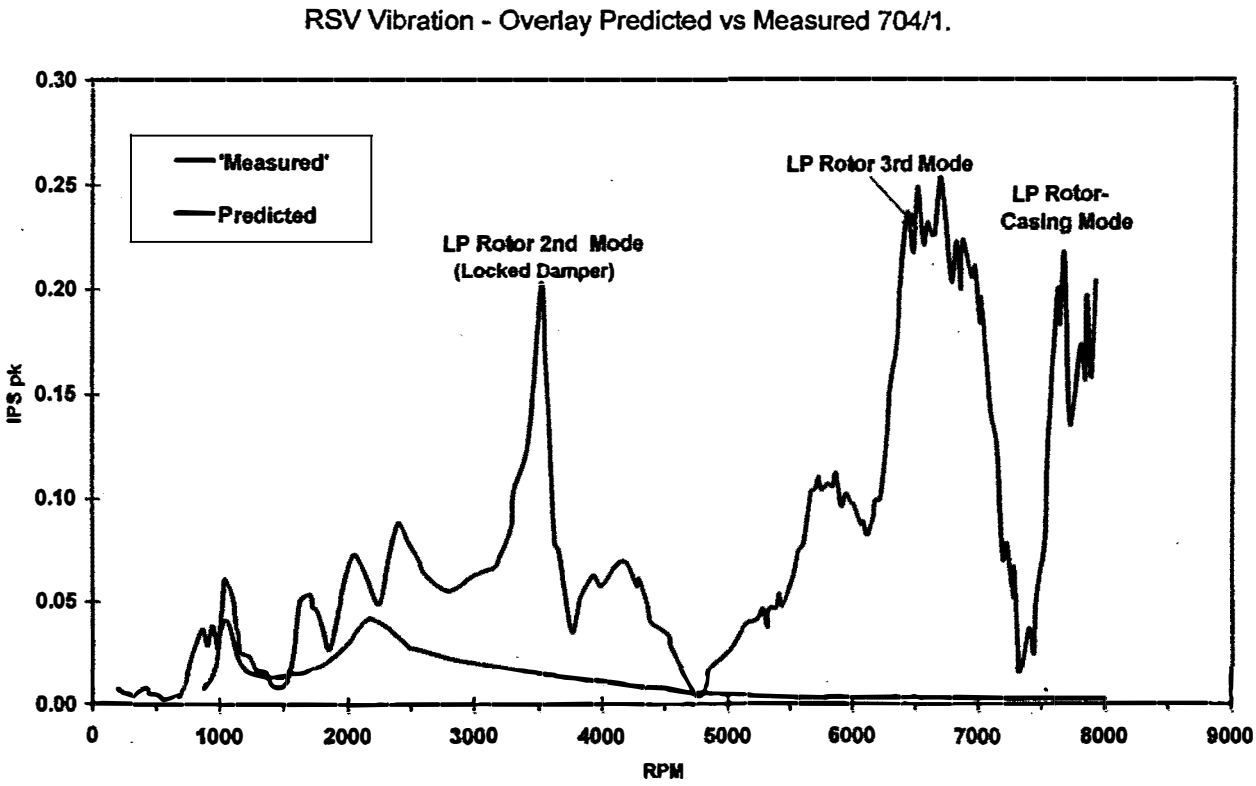

Figure 3. Comparison of Experimental Engine Vibrations and Predicted Response at Vertical Rear Support (RSV)

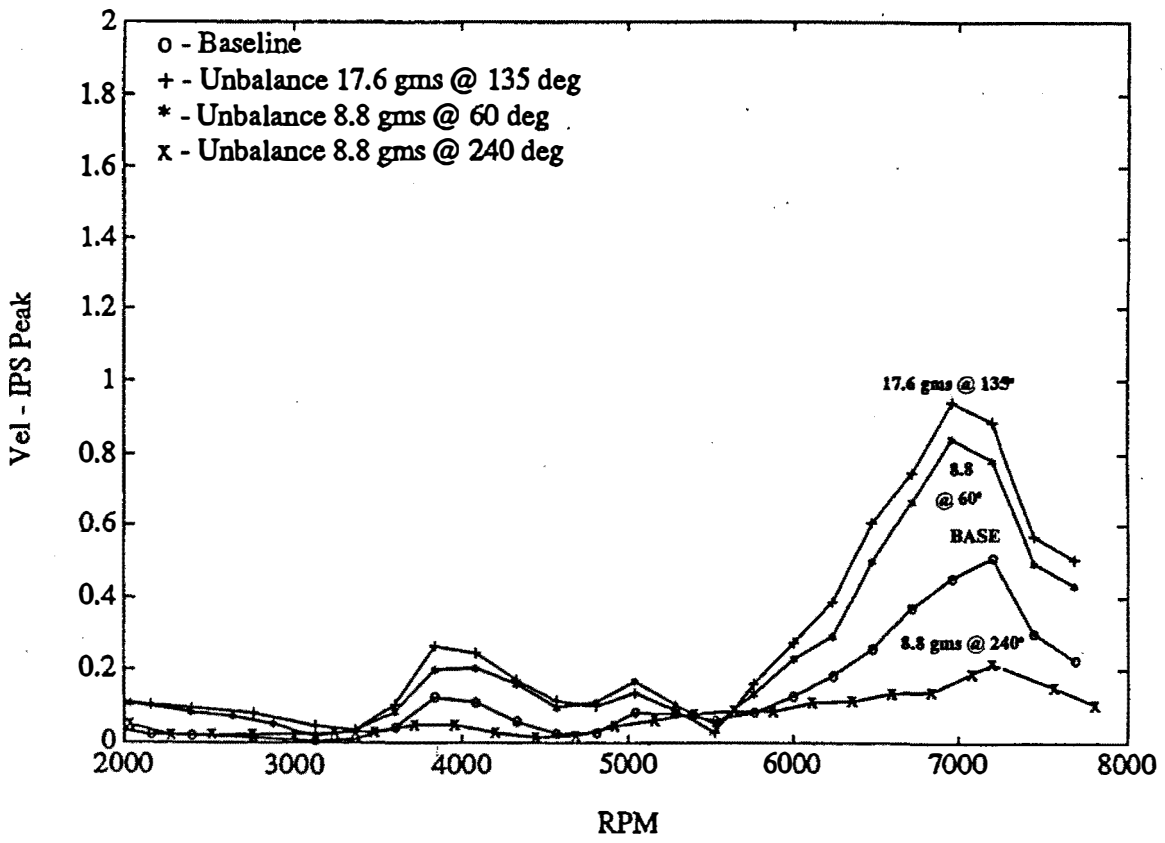

Figure 4. Engine Vibrations at Far Front Frame (*FARVFF*) For Various Values of Fan Unbalance

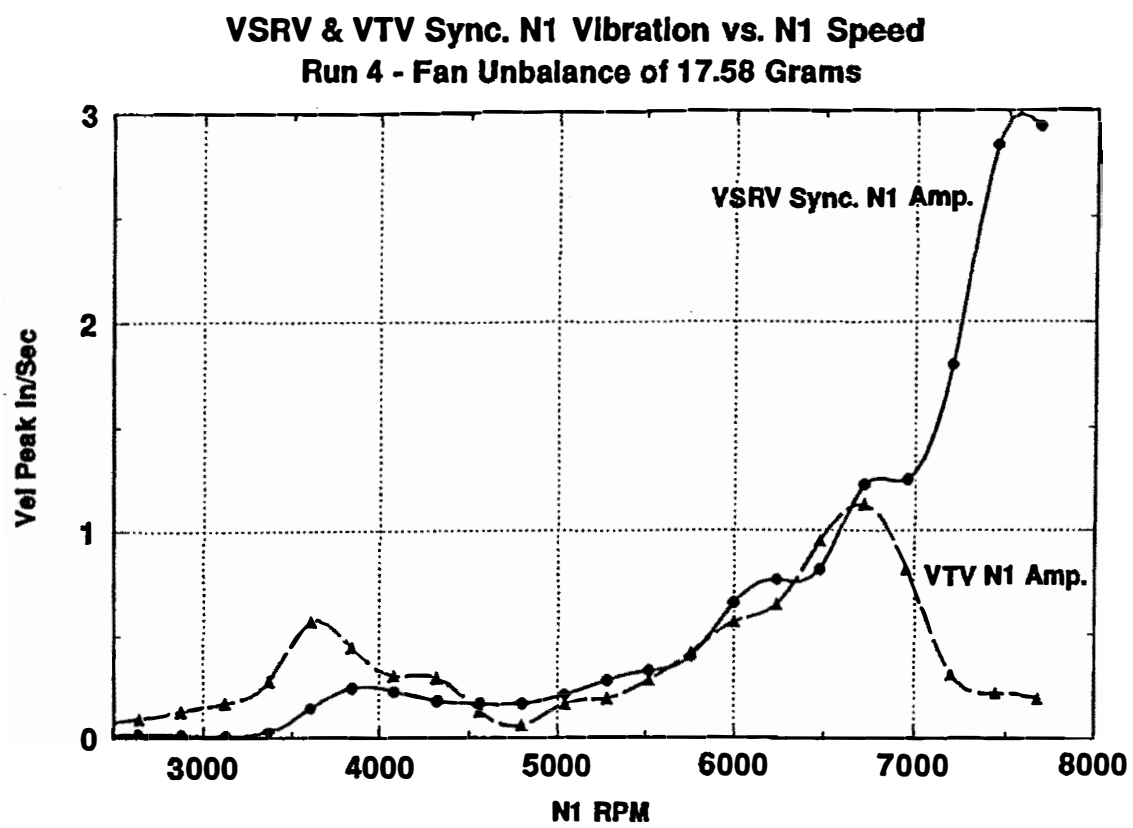

Figure 5a Engine N1 Vibrations at Rear External Vertical Casing Support (VSRV) and Internal Vertical Turbine Casing (VTV) With 17.6 Grams of Fan Unbalance

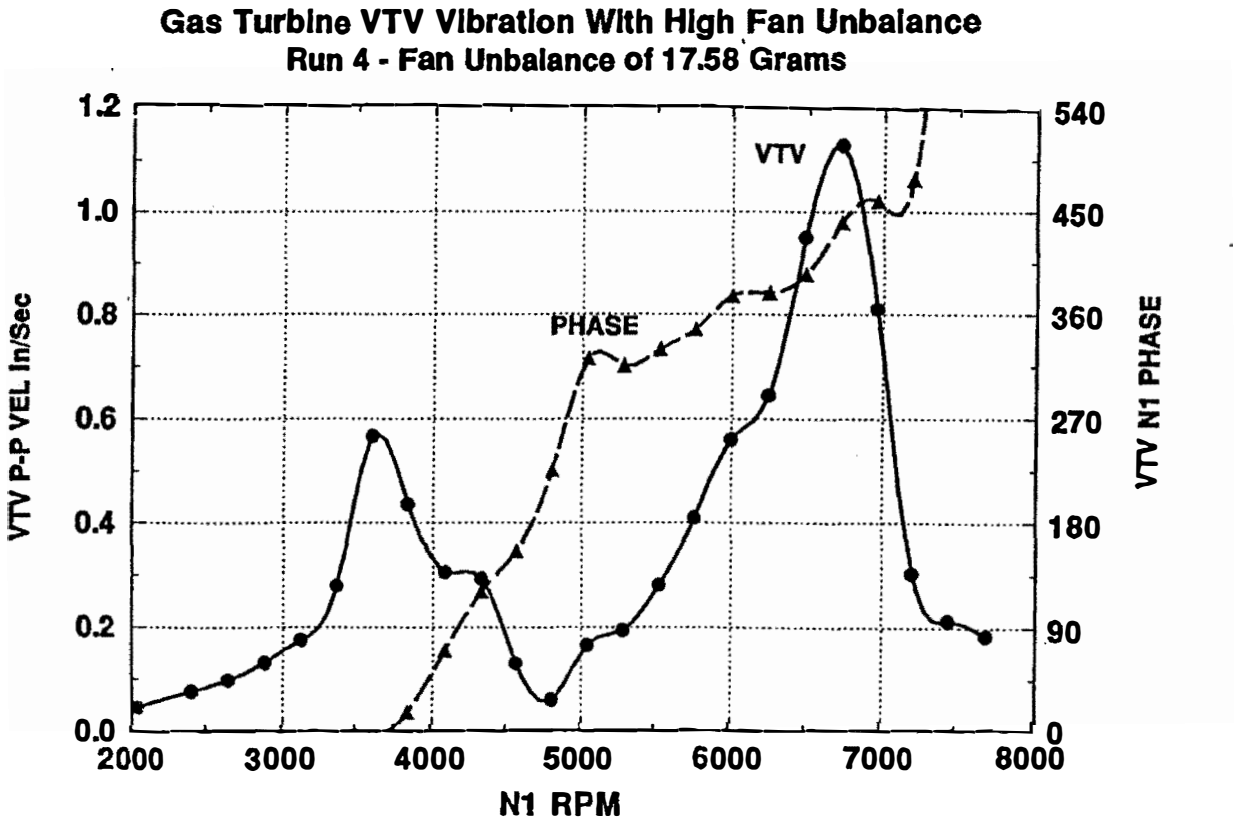

Figure 5b Engine N1 Vibrations at Internal Vertical Turbine Casing (VTV) With 17.6 Grams of Fan Unbalance

2. Low Pressure Turbine Critical Speed and Damped Eigenvalue Analysis

From the experimental investigations of the influence of fan unbalance on the engine response, a study of the critical speeds of the low pressure turbine were initiated. The results of the low pressure turbine critical speed analysis were first reported by Park, Gunter, and Fang in the March 1994 paper, *Vibration Analysis of a Jet Aircraft Engine*, at the University of Virginia. In the initial analysis, a model similar to the manufacturer was used for the computation of the critical speeds. The third critical speed was placed above 11,000 RPM by this model. The early analysis of the LP turbine at the University of Virginia indicated that the gyroscopic moments of the 3-stage turbine section has a profound influence on the location of the LP turbine third critical speed.

For illustration purposes, a 9,000-element finite element model of the LP turbine was generated using ***ALGOR***, as shown in Figure 6. Figure 7 represents a 3-dimensional view of the finite element turbine model. Figure 8 represents the cross-sectional drawing of the LP rotor at the turbine location. The turbine assembly is a 3-stage turbine configuration which is bolted onto the conical section of the main LP rotor. The construction of the bolted-up conical turbine section leads to many questions as to the overall stiffness of the assembly.

Figure 9 is a detailed finite element model of the LP rotor section showing the turbine construction. In this finite element model, the turbine blades are attached to the disk station. When the turbine blades are assembled in the disk, the blades have a certain amount of initial clearance. As the turbine reaches the operating speed, the blades lock into the turbine disk fir tree. There is a gyroscopic reduction in the turbine total effective polar moment of inertia due to the fir tree effect and the fact that the blades are flexible and not rigidly attached to the disk. Another consideration of flexibility in the system is that the turbine section is bolted, rather than welded, onto the LP rotor. This leads to moment release in the system, which can cause a further degrading of the gyroscopics. When the original LP rotor critical speeds were predicted by the manufacturer, the entire turbine section was treated as a single plane with lumped polar and transverse moments of inertia equivalent to the three disk stations. The assumption of a rigid single disk to represent the turbine section leads to a greatly elevated third critical speed.

Figure 10 represents the cross-section of the LP gas turbine rotor treated as a two-level system. The LP rotor was modeled using the ***DyRoBeS***© finite element rotor program. The turbine section is connected to the LP rotor by means of radial and angular springs. This provides for the examination of moment release between the turbine and the LP shaft. In addition, the LP rotor model, as shown in Figure 10, also has incorporated into it bearing support masses at the three bearings. Of particular significance is the influence of support mass at the turbine location. A turbine bearing support mass of .3 9 (16 lb) was assumed in order to examine the characteristics of turbine foundation mass on the dynamic characteristics of the LP turbine.

Figure 11 represents the effect of reduction of polar moment of inertia on the third critical

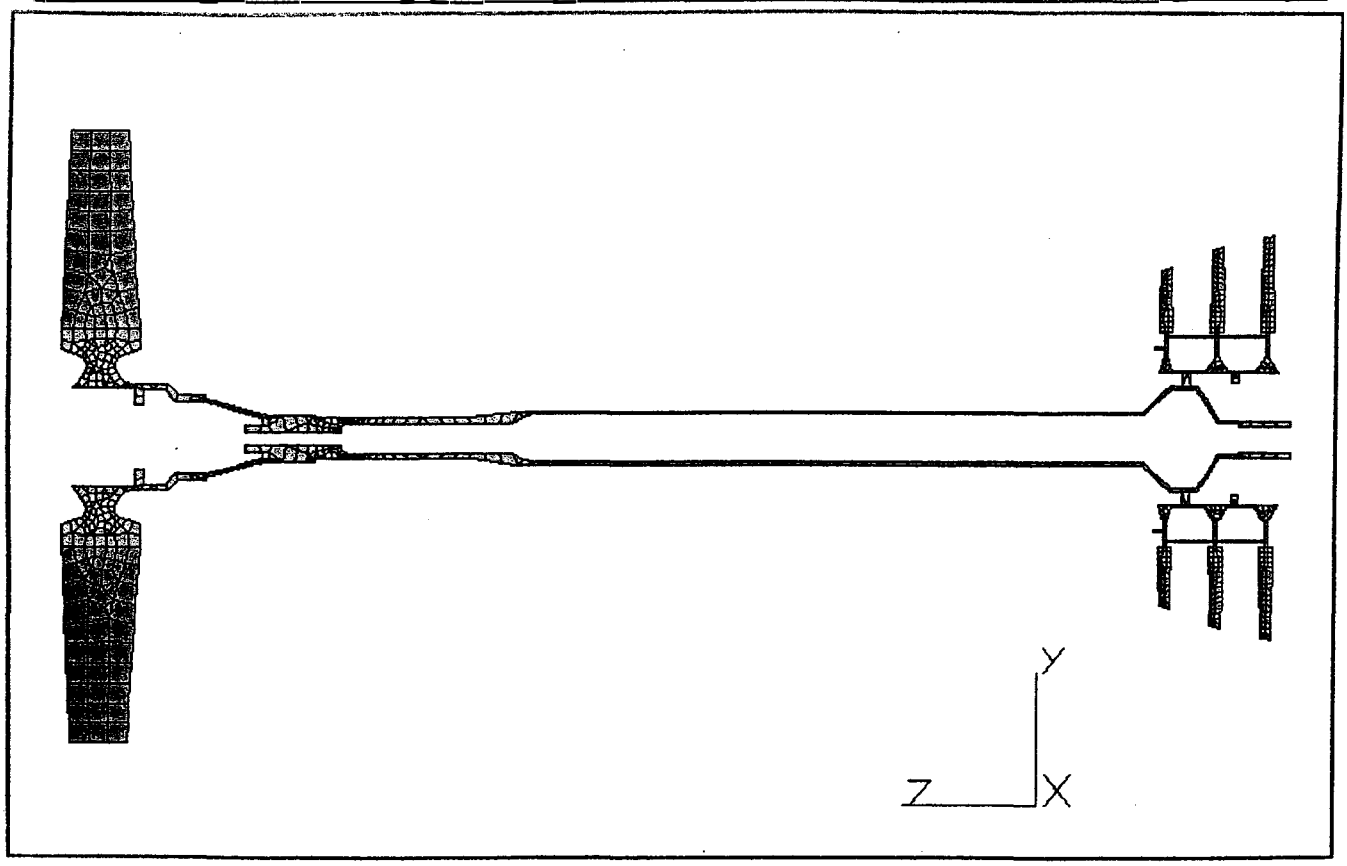

Figure 6 Cross-Sectional View of LP Rotor

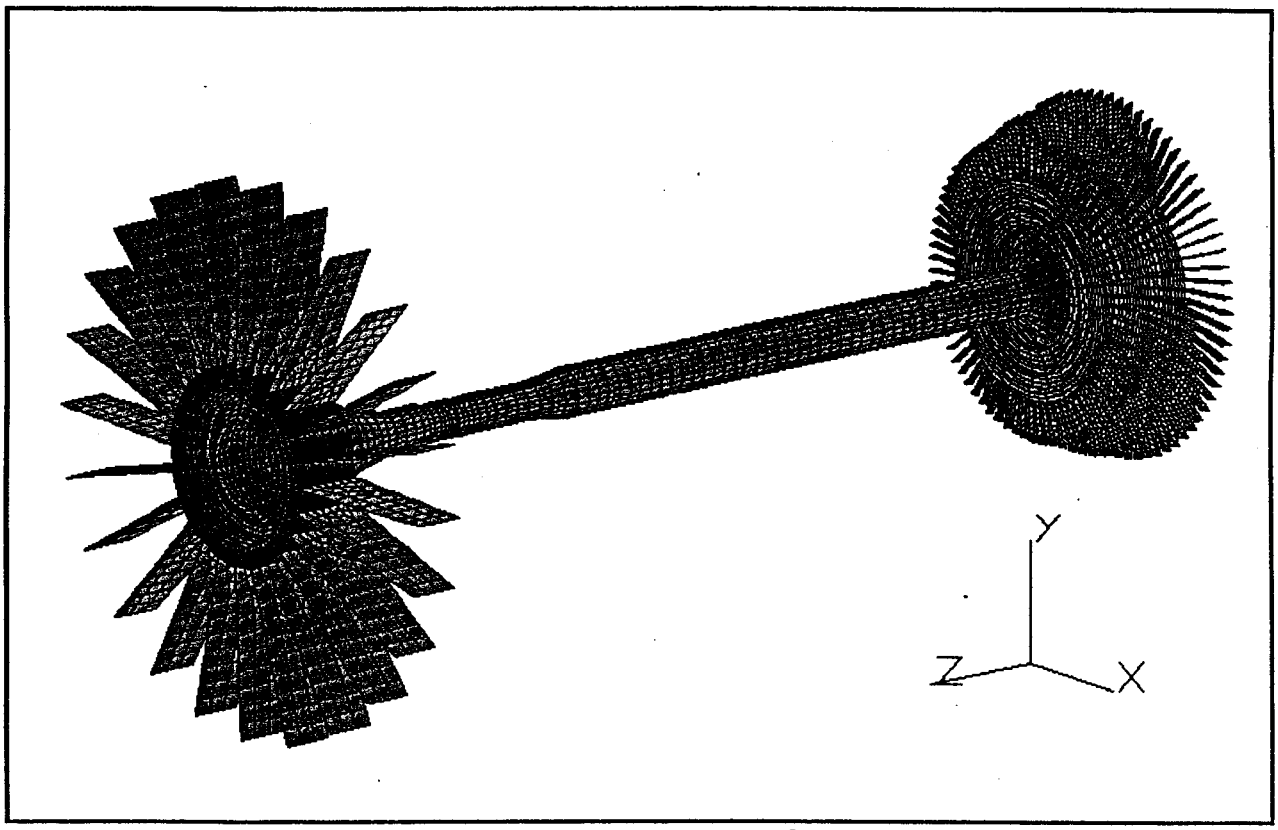

Figure 7 3 Dimensional Finite Element Model of LP Turbine using ALGOR

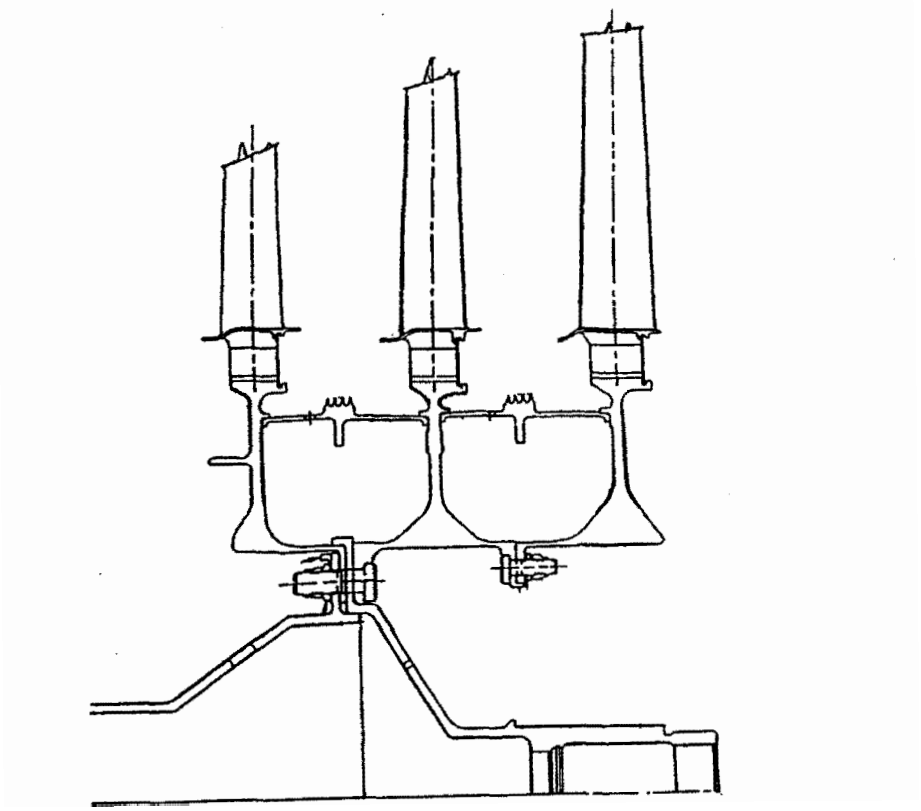

Figure 8 Cross Sectional Drawing of LP Rotor at Turbine Location

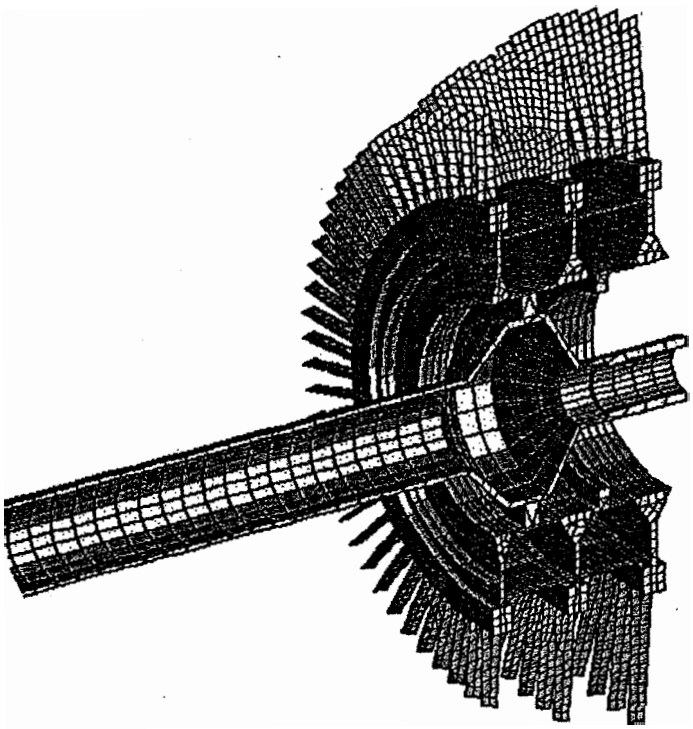

Figure 9 NASTRAN Finite Element Model of LP Turbine Showing Turbine Section

Figure 11 represents the effect of reduction of polar moment of inertia on the third critical speed, in which the turbine section is treated as a single disk. The turbine third mode is extremely unusual in that at zero speed, the planar third mode is at 6,000 RPM. If the turbine section is treated as rigid, then the third critical speed increases to 12,000 RPM at running speed. This is called the synchronous critical speed. In actuality, the various effects of disk flexibility and looseness of the blades combine to cause a reduction in the effective polar moment of inertia. In this model it is seen that as the polar moment of inertia is reduced to 50%, the third critical speed drops to around 8,000 RPM. A further reduction in the third critical speed is obtained by a more detailed modeling of the turbine section as a two-level rotor.

Figure 12 represents the turbine third mode with turbine mass support = .3 and a moment release rotational stiffness of 1.0E7 in-lb/rad connecting the turbine to the LP shaft. Note that the turbine third mode has dropped from 12,000 RPM to 6,535 RPM, as shown in Figure 12. Also note that the fan station runs about its inertia axis. Large values of unbalance placed at the fan cause forces transmitted though the main number 2 bearing into the engine casing and intermediate structures. Of particular interest is the slope of the shaft at the turbine location. The LP rotor is highly susceptible to couple or moment unbalance at the turbine area. A moment or couple unbalance in the turbine area may be generated simply by the process of bolting the turbine section onto the LP rotor. Therefore, it is essential that the turbine area be separately two-plane balanced and that the angular run-out of the turbine during assembly be minimized. If this is not done, then it is impossible to trim out the engine by placing a single-plane correction at the fan location. The turbine area cannot be accessed for field balancing and for large values of turbine couple unbalance, the engine must be removed from the aircraft and balanced at the factory.

Figure 13 represents the turbine fourth mode at 7,945 RPM with turbine foundation mass = .3. Note that the mode shape for the fourth turbine mode is almost identical to the mode shape as shown in Figure 12 for the third mode. This is referred to as a bifurcated mode and is caused by the introduction of foundation mass. In the first case, the foundation mass is acting in phase to the bearing motion, and in the second case, the foundation mass is acting out of phase. Note that in Figure 13 there is a slight deviation between the slope of the turbine and the LP rotor shaft. This is due to the influence of the rotational spring, which causes some moment release.

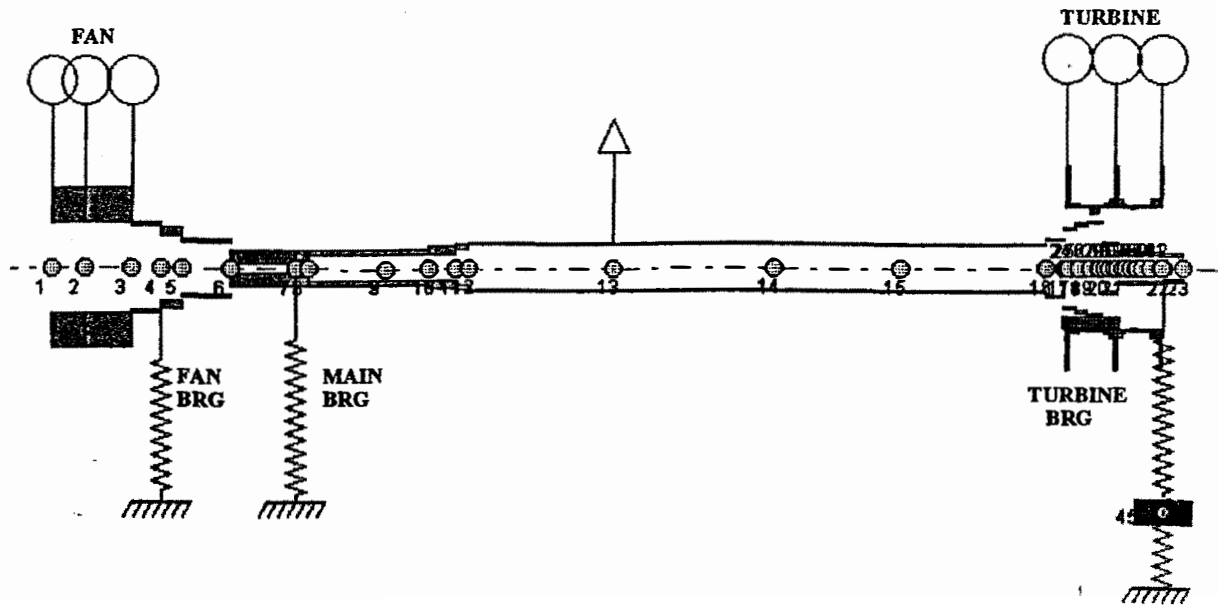

Figure 10 Cross Section of Two Level LP Gas Turbine Rotor Including Bearing Support Mass and Moment Release Using *DyRobes* Finite Element Rotor Program

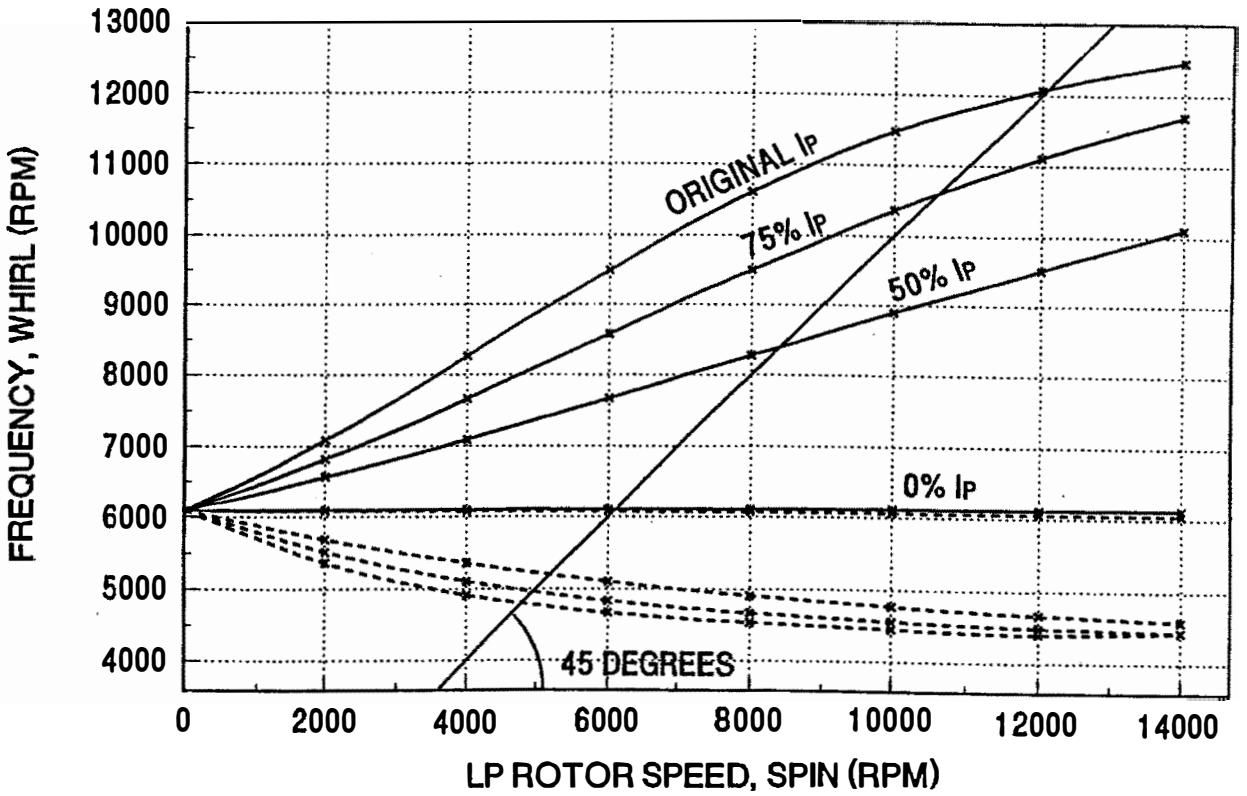

Figure 11 LP Rotor 3rd Synchronous Critical Speed Vs RPM For Various Turbine Polar Moment of Inertia Ip Values

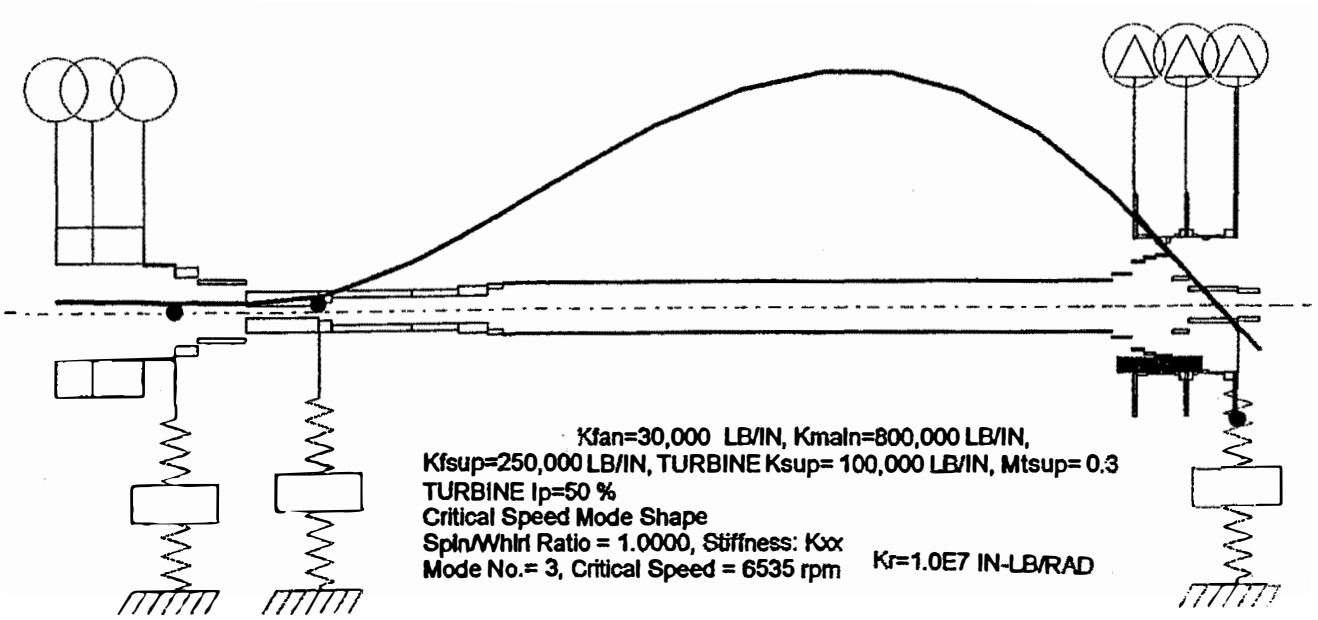

Figure 12 Turbine 3rd Mode at 6,535 RPM With Turbine Bearing Support Mass =0.3
(50% Turbine Gyroscopic Effects)

Kfan=30,000 LB/IN, Kmain=800,000 LB/IN, Kt= 50,000 LB/IN,Kr=1.0E7 IN-LB/RAD,
Kfsup=250,000 LB/IN, TURBINE Ksup= 100,000 LB/IN, Mtsup= 0.3 , Cfan=15 LB-S/IN, Ctur=20

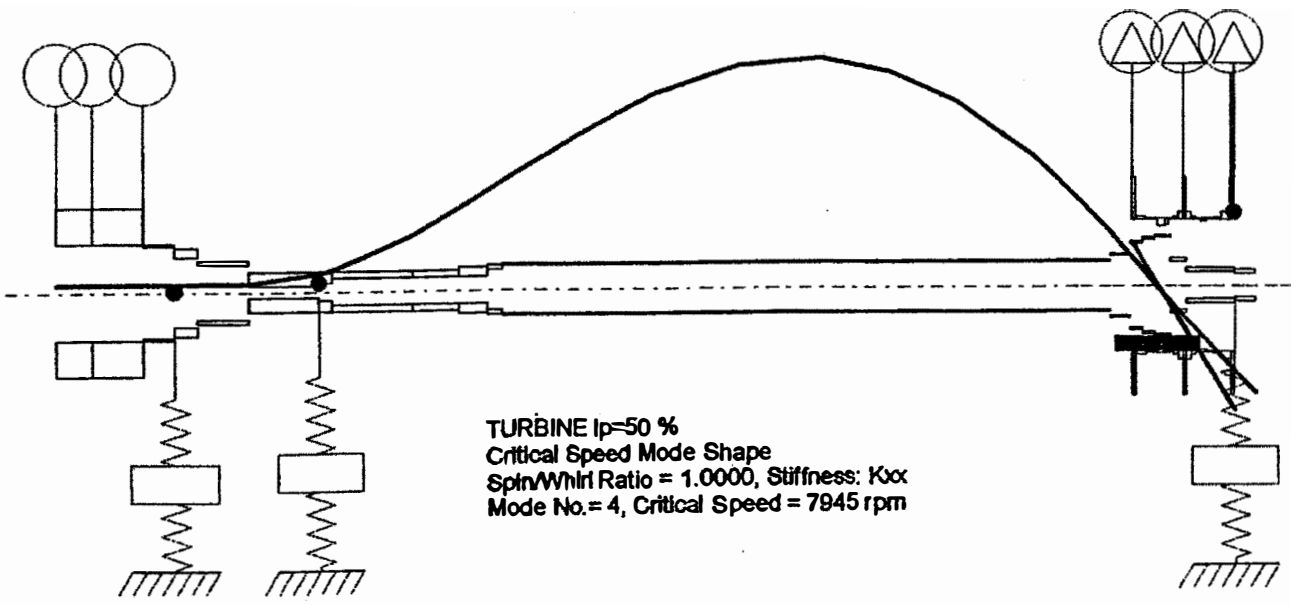

Figure 13 Turbine 4th Mode at 7,945 RPM With Turbine Bearing Support Mass =0.3
(50% Turbine Gyroscopic Effects)

LP Damped Mode Shapes

Figure 14 represents the third forward, damped LP turbine mode, including damping at the fan and turbine locations. Because of the small motion at both the fan and the turbine damper locations, the amplification factor is 17. It is of interest to note that theoretically increasing the squeeze film damping value does not cause a significant reduction in the rotor amplification factor. Therefore, from the damped eigenvalue analysis, it can be surmised that the turbine is very sensitive to turbine radial and, particularly, moment unbalance.

Figure 15 is the fourth forward, damped LP turbine mode at 7,847 RPM. As previously stated for the undamped critical speed, the damped forward fourth mode is identical in appearance to the third mode. However, the amplification factor for the fourth mode is 13, as compared to 17 for the third mode. The reason for this is that the motion of the foundation is out of phase to the bearing in the fourth mode. This makes the squeeze film damper somewhat more effective than in the third mode. In general, a bifurcated upward mode normally has higher damping than the lower mode, in which the foundation is moving in phase with the bearing.

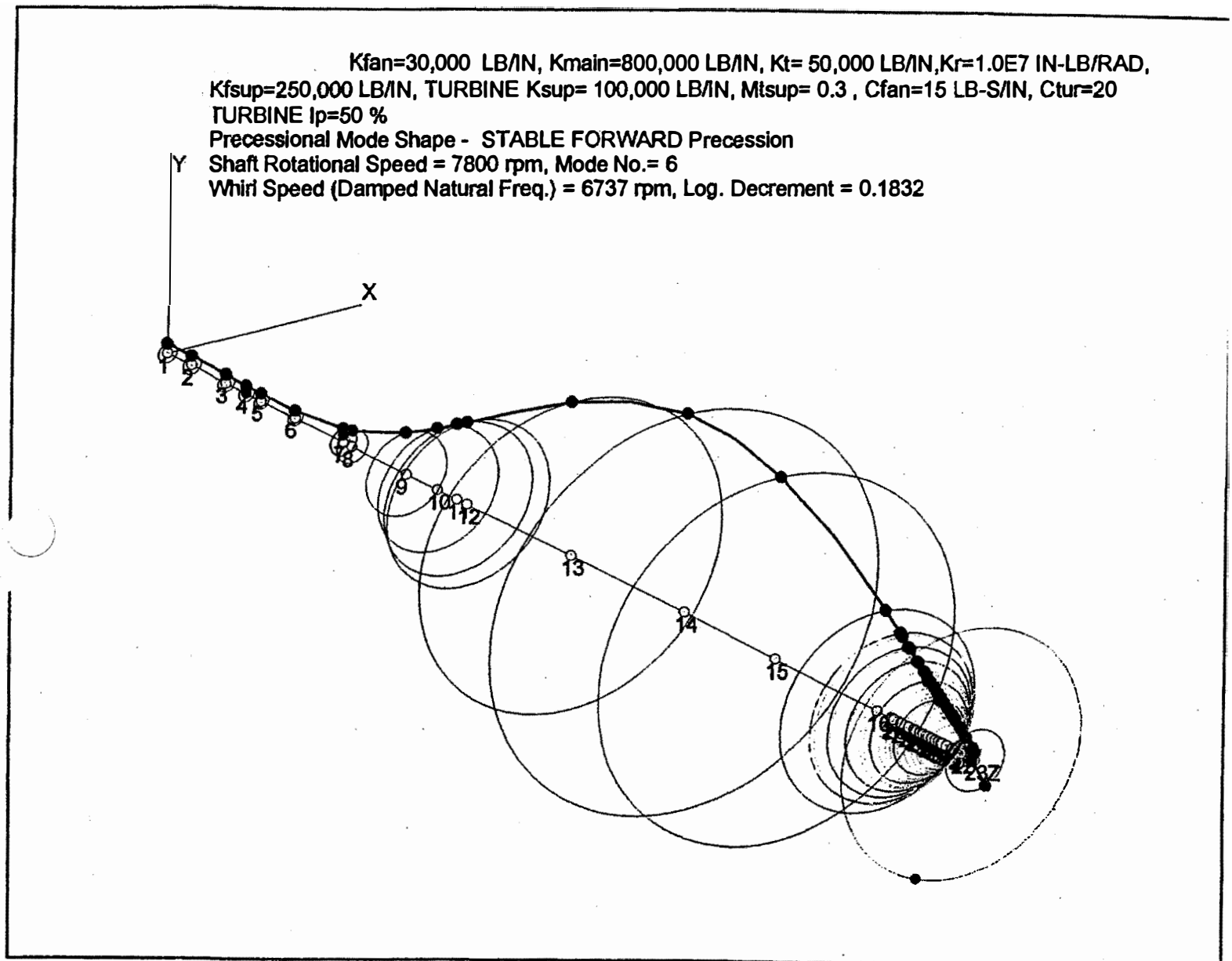

Figure 14 3 rd Forward Damped LP Turbine Mode at 6,737 RPM (112 Hz) , Log Dec= 0.1832, Ac=17

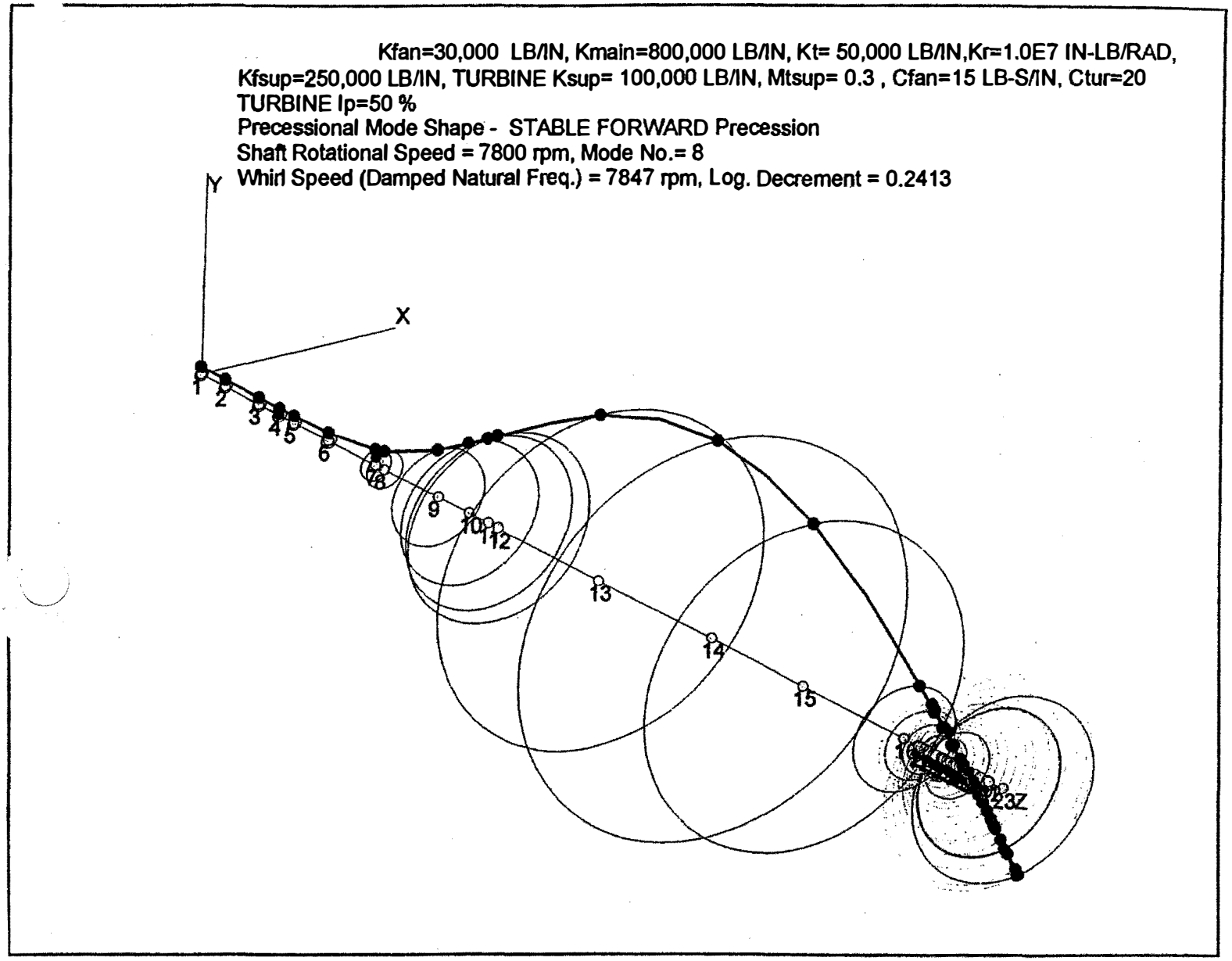

Figure 15 Forward Damped LP Turbine Mode at 7,847 RPM (130 Hz) , Log Dec= 0.241, Ac=13

3. Rotor Casing Finite Element Analysis

In the first modeling of the gas turbine engine, a finite element beam model for the rotor was considered. The casing was assumed to be simple lumped masses attached at the bearings. Although this provided a great deal of physical insight into the dynamical behavior of the engine, it was felt that such an analysis was too simplistic to explain the complicated rotor-casing shell modes observed experimentally. Because of the light construction of aircraft gas turbine engines, casing modes may be excited in the operating speed range. Figure 16, for example, represents an engine casing mode at 128.9 Hz, based on the proprietary finite element shell code of the engine manufacturer. The analysis of the dynamical characteristics of a jet engine is complicated by the internal structure. For example, Figure 17 represents the front and rear bearing supports and intermediate casing. This component has a resonance frequency of 121.5 Hz. However, in the casing modeling performed by the manufacturer, the low pressure and high pressure rotors were not included in the analysis.

In order to model the aircraft engine, the individual components were first modeled by R. Armentrout in ***ALGOR*** on the PC computer. These components were later transferred into the ***MSC/NASTRAN for Windows*** program for further analysis. It was found that the ***NASTRAN*** program could compute frequencies 15 to 20 times faster than ***ALGOR***. Figure 18, for example, represents the cross-section of the front bearing support, as generated by ***NASTRAN***. The ***NASTRAN Windows*** PC program uses the commercial modeler ***FEMAP*** for input and output. The ***FEMAP*** interface has the added advantage that it may translate between the various commercial finite element packages.

Figure 19 represents the ***NASTRAN*** model of the rear bearing support frame. Note the external tabs, or lugs, for the rear engine mounts. It was later determined that increasing the flanging in this area would greatly stiffen the casing modes excited in the operating range. After all the individual bearing support and casing components were initially modeled by Armentrout in ***ALGOR***, they were assembled and translated into ***NASTRAN*** for computations. A typical system mode is shown in Figure 20, with a rotor casing mode at 123 Hz. Note that there is considerable rotor-casing interaction in this mode shape. Forced response was computed using a direct solution method and also by a modal method. The modal method proved to be 50 times faster than the direct solution. However, a care must be taken in selecting the modes to at least three times the operating speed range. This required the inclusion of several hundred system modes. The extensive finite element models and mode data generated were saved on a Jazz drive with 2 gigabytes of storage.

Based upon the various unbalance runs generated, Dr. R. Navaneethan, of Cessna, combined the theoretical analysis of several unbalance distributions to generate the produce the response, as shown in Figure 21. In order to produce the experimental match, it was necessary to degrade the gyroscopic moment by 50% in the LP turbine.

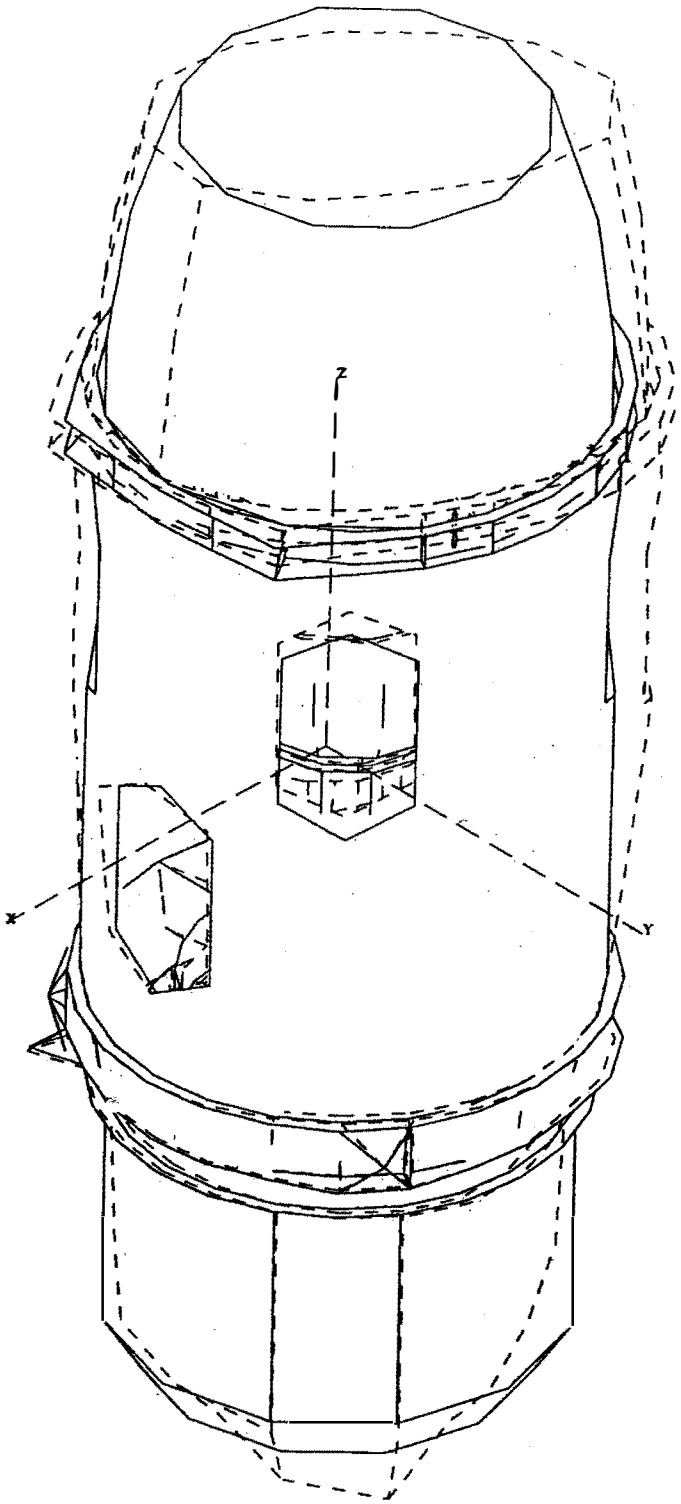

Figure 16 Engine-Casing Two-Lobed Shell Mode at 128.9 Hz - Mode No. 32

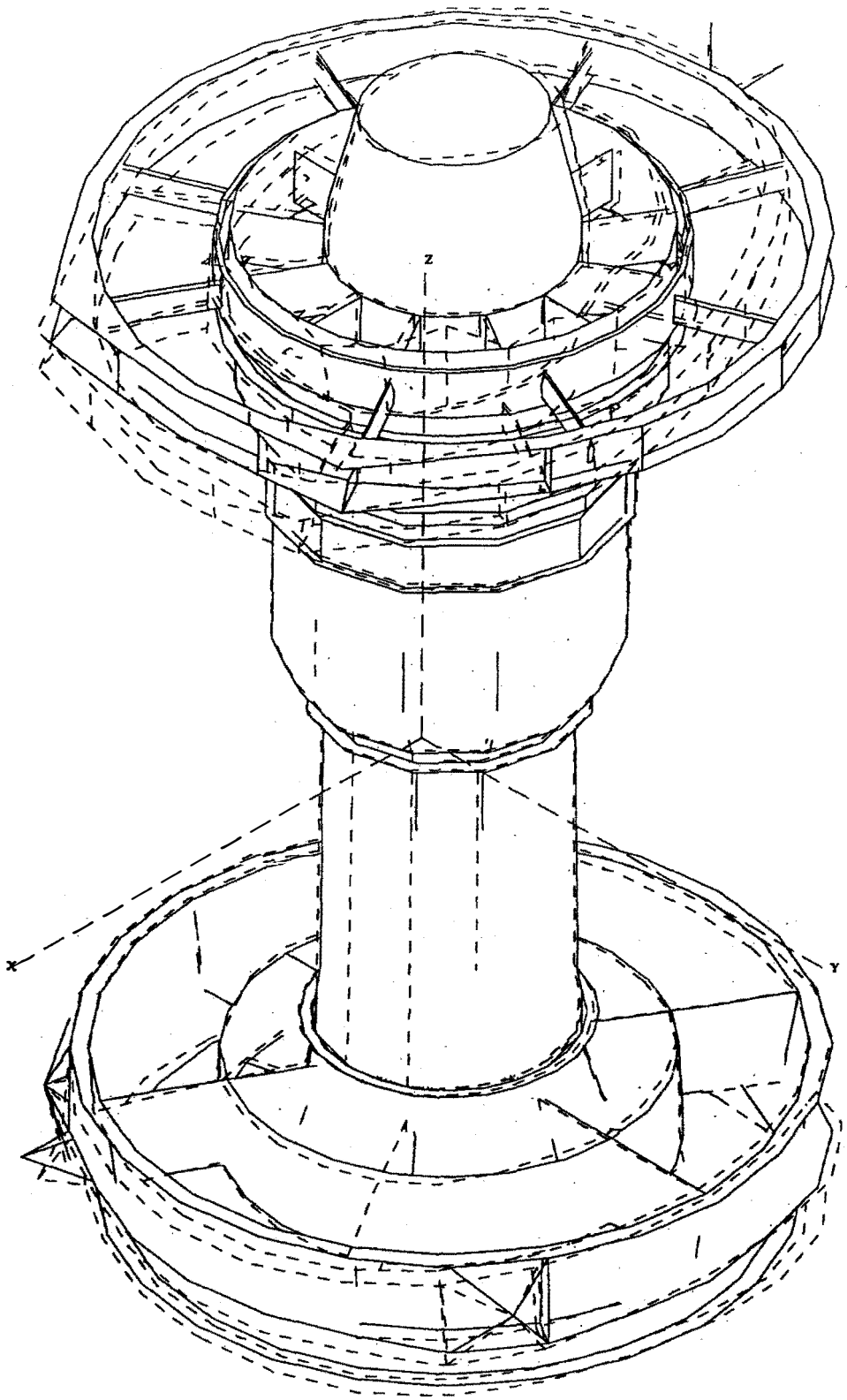

Figure 17 Front and Rear Bearing Supports (With Engine Mounts) and Intermediate Casing Natural Frequency at 121.7 Hz

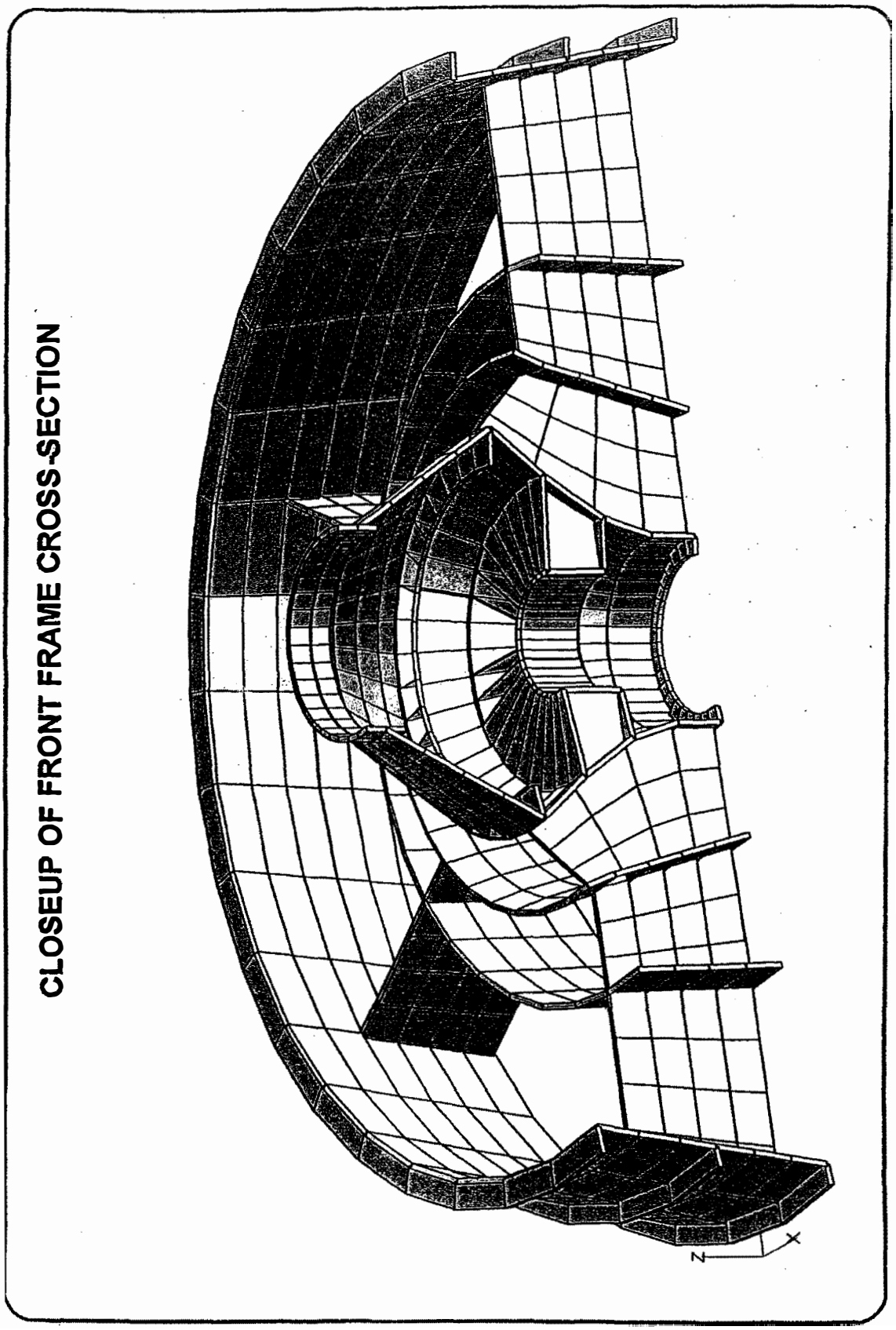

Figure 18 Cross-Sectional View of *NASTRAN* Model of Front Frame

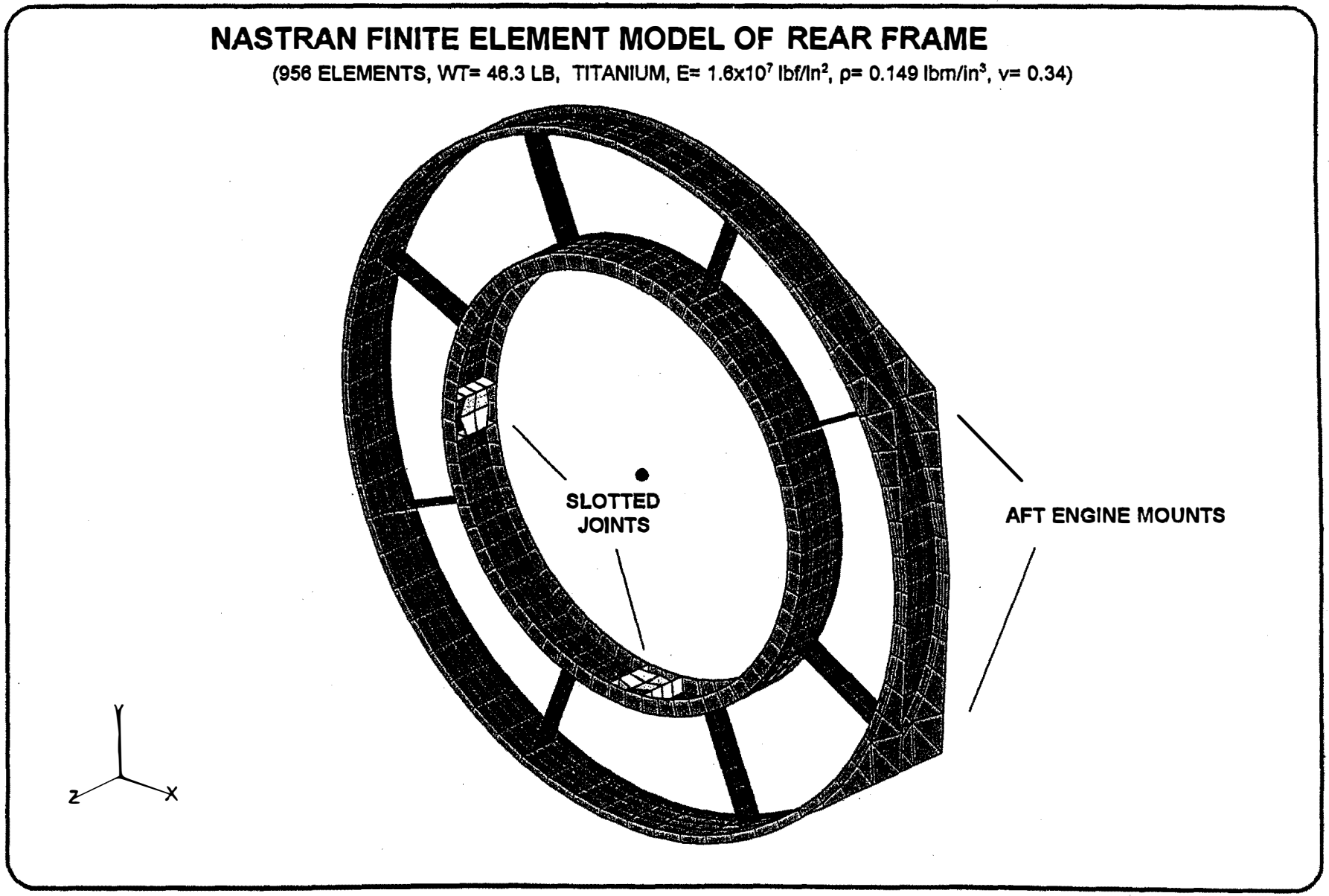

Figure 19 ***NASTRAN*** **Model of Engine Rear Frame**

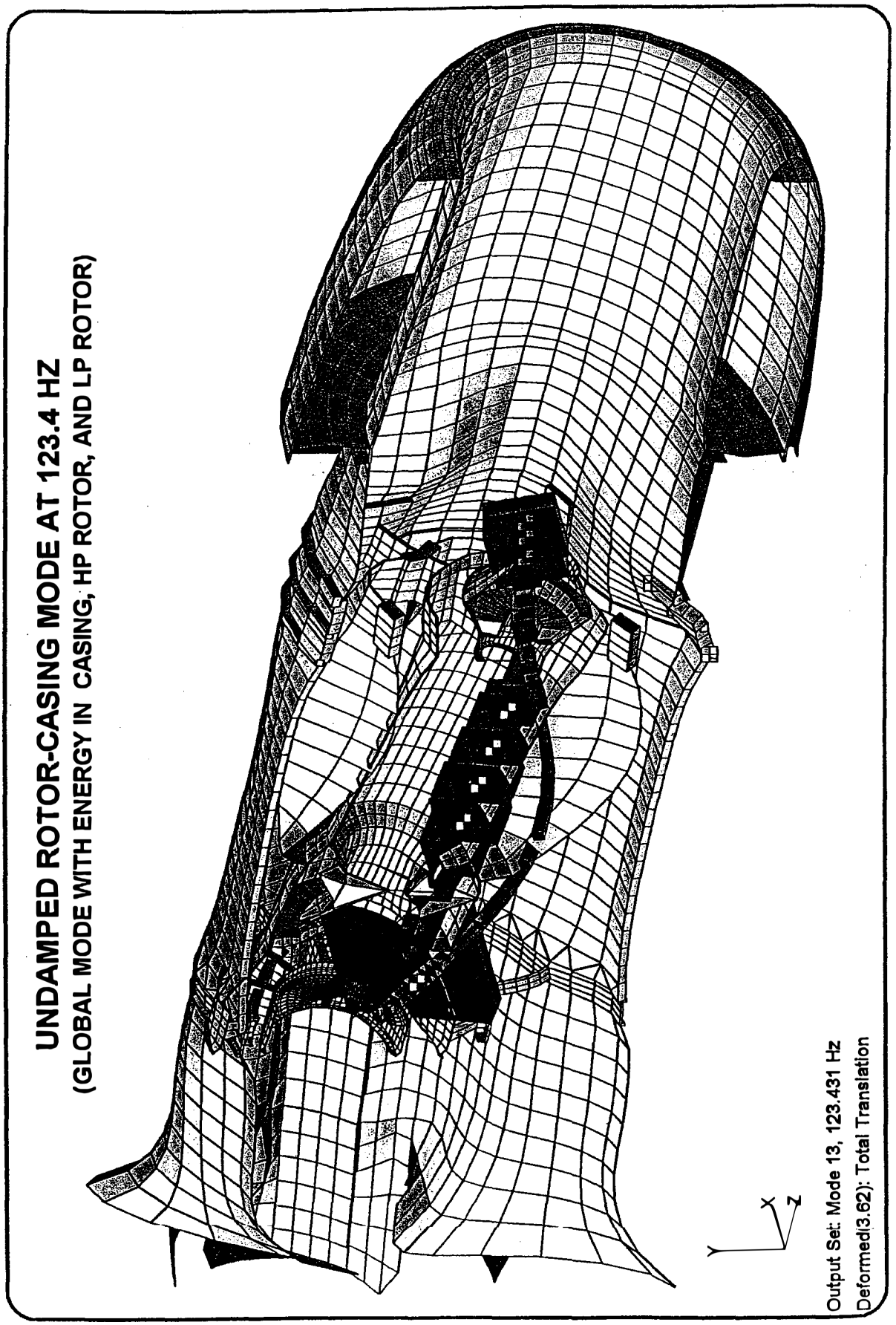

Figure 20 Undamped Rotor-Casing Mode at 123.4 Hz

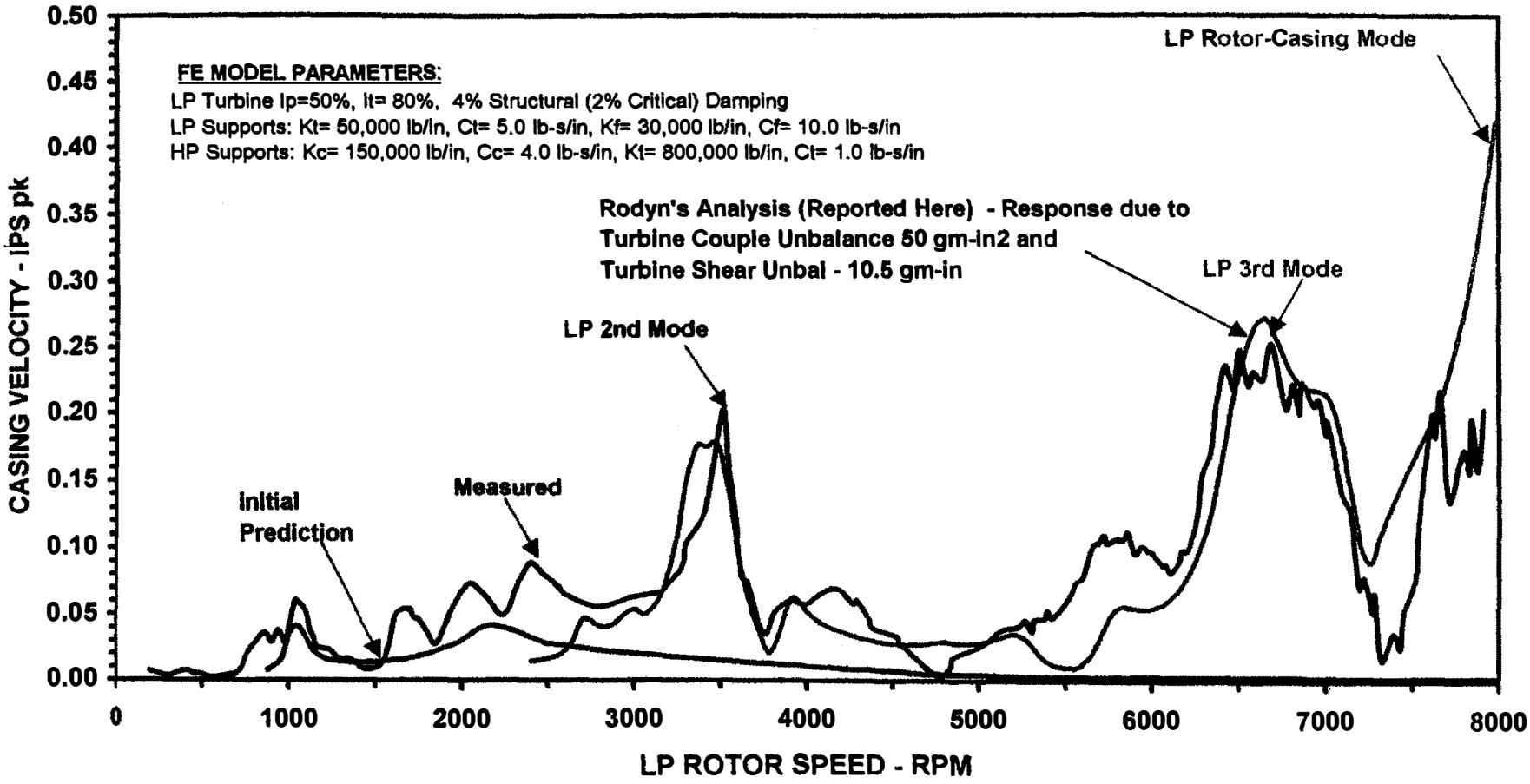

Figure 21 Comparison of RSV Vibration - Measured, Original, and Final FE Model Prediction Test Inlet Bell and Test Exhaust Nozzle - 50% LP Turbine Gyroscopics

4.1 Factory and Test Balancing

In order to minimize problems of balancing in the test cell and trim balancing in the field, initial component balancing must be carefully done before the engine reaches the test cell. The engine is particularly sensitive to single-, and especially turbine-, couple unbalance. Hence, attention must be placed on careful component balancing of the 3-stage turbine assembly. Analysis shows that it is impossible to correct by single-plane balancing of the fan only, for even a moderate amount of turbine moment unbalance. This turbine unbalance couple may be caused by two turbine stages with unbalance weights placed 180° out of phase, or by a skew of the turbine assembly. A run-out face check should be made on the turbine assembly to check for skewing of the assembly.

Figures 22 and 23 represent a comparison of the best PBS balance with the steel test nozzle and the thrust reverser installed. The test nozzle is a heavier component composed of steel. It causes a very high amplification mode around 125 Hz that is not present when using the lighter engine thrust reverser, which also appears to have more damping.

In Figure 22, RST represents a translational motion at the rear of the engine. In the test facility, the engine is supported from the top. On the aircraft, the engine is attached horizontally to the fuselage. The large peak observed in the test facility is a torsional mode at 108 HZ which does not occur on the aircraft. When the engine is balanced to reduce this vibration in the test stand, the actual engine in service may appear to be badly balanced. Hence, the RST vibration signal must not be used for balancing.

In Figure 23, which shows a comparison between the steel test nozzle and the engine thrust reverser, it is apparent that the test nozzle has higher amplification factors at 93 Hz and 125 Hz. When using the test configuration, the balancing data should be between 85 Hz and 115 Hz. The data above 120 Hz should not be used, as this would distort the balancing due to the presence of the nozzle mode at 125 Hz. This nozzle mode is similar to the ringing of a bell.

Superior balancing is obtained when the balancing is based upon using the actual engine thrust reverser. The steel test nozzle places a bell mode at 125 Hz. In all cases, the balancing process should concentrate on balancing between 85 and 120 Hz. High engine response above 120 Hz does not excite the cabin modes or sound pressure level (SPL), which is resonant around 6,800 to 7,000 RPM (113 to 116 Hz).

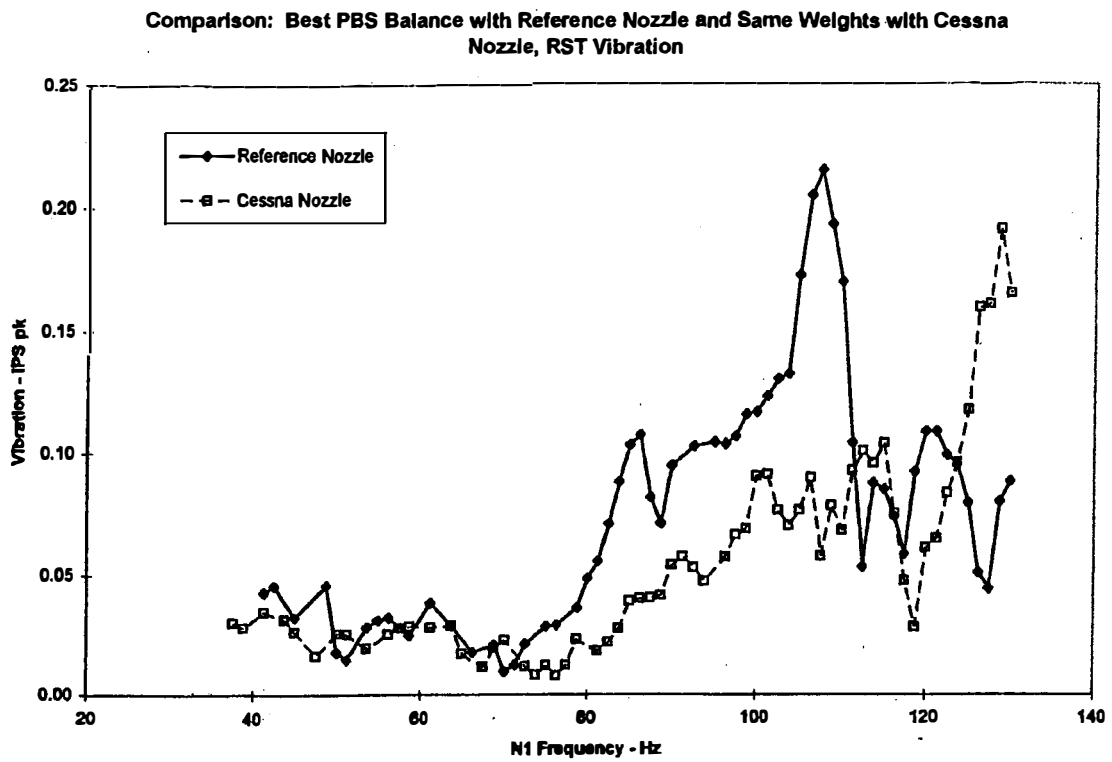

Figure 22 Comparison of RST Between Test Exhaust and Engine Thrust Reverser Nozzle With Best Least Squared Error Balancing

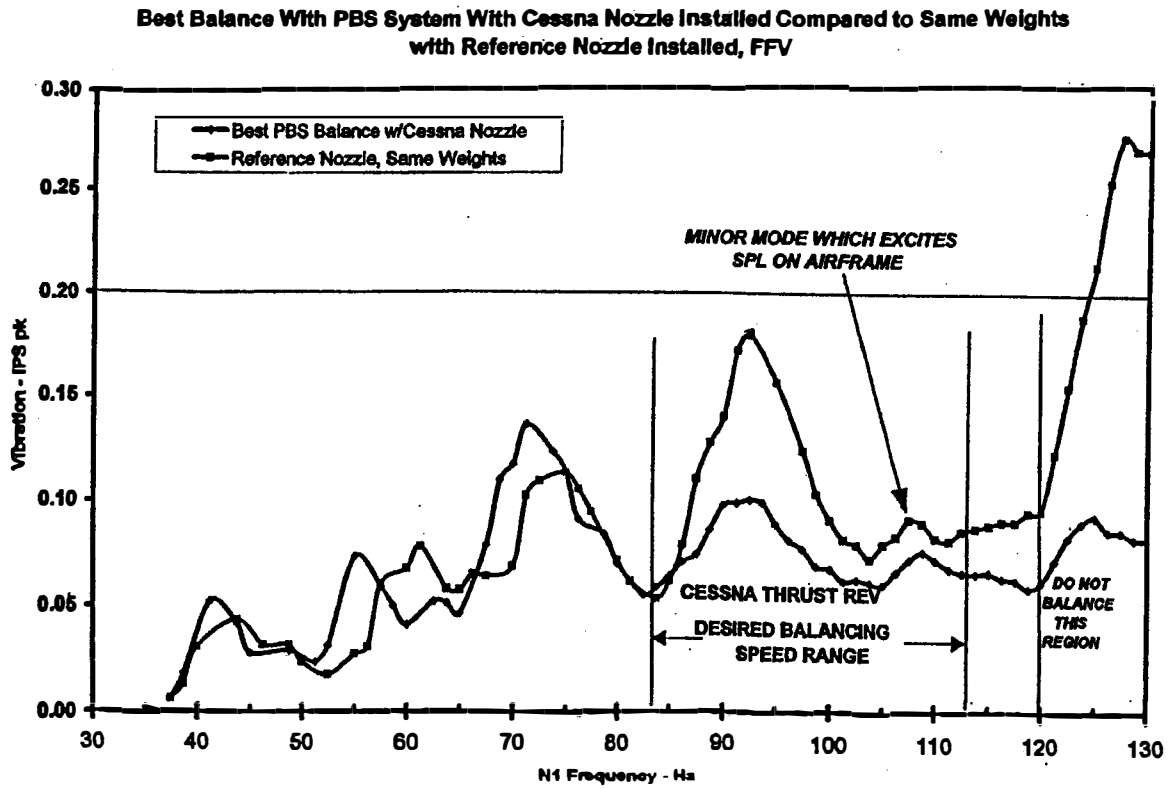

Figure 23 Comparison of FFV Between Test Exhaust and Engine Thrust Reverser Nozzle With Best Least Squared Error Balancing

4.2 Three Trial Weight Method of Balancing

Limitations of Single-Plane Balancing By the Influence Coefficient Method

For the case of high engine vibration levels or high SPL (sound pressure level) in the cabin, the only practical plane available for balancing is single-plane on the fan of the LP rotor. For cases in which one does not have large turbine unbalances, then fan balancing may be done to reduce engine vibration levels and the cabin sound pressure level (SPL). The problem with single-plane fan balancing on the aircraft are that one single plane of balance can not reduce all levels of vibration, particularly in the case when there is a number of modes present. When multiple vibration signals are used over a speed range, then the least-squared-error balance is a compromise based on all the readings. The balance correction predicted is always reduced when additional vibration data is added to the computation.

Single-plane field balancing on the aircraft by the least-squared-error method requires an accurate phase reference signal. Since there is not a convenient timing signal probe on the engine, a laser reference beam is often used to obtain phase. Under certain conditions of high humidity, it is not possible to obtain an adequate signal for phase. Without accurate phase measurements, balancing by the influence coefficient method may be very time consuming and actually take more time then the two- or three-run balancing method without phase. On should also be reminded that, even under the best of circumstances with accurate phase measurements, it is very easy to misplace the balance weights because of the phase convention and method of labeling the balance holes. Under pressure to quickly perform a balance and return the aircraft to operation, it is easy to place the balance weight in the wrong quadrant, or 180^0 out of phase. In the case where a balance weight has to be moved to another location, is a perfect opportunity to apply the two- or three-run method using polar plots.

Advantages of 3 Trial Weight Method of Balancing

The two- or three trial weight method of balancing has certain advantages over the influence coefficient method, providing that weights may be easily added or removed . Some of these advantages are as follows:

1. No phase measurements are required
2. Vibration data does not have to be exactly at the same speed
3. Balancing may be calculated based on the maximum amplitude at a critical speed
4. Accurate balancing may be performed with only two trials
5. The first trial weight will usually provide an indication as to the next balance locations.

6. Direction of rotation is immaterial
7. Placement of the balance weights is foolproof
8. Accurate balancing may be obtained even for highly nonlinear systems.
9. The method may be based on peak values at an engine or cabin resonance conditions using a spectrum analyzer.
10. If trial weights can be quickly moved, the method is very fast.
11. If the method will not balance out a particular mode (such as SPL at 115 Hz, for example), then the influence coefficient method will also not work.
12. If balance is unsatisfactory using this method, then the engine should be removed and returned to the factory for rework.
13. Sensitivity coefficients may be developed (equivalent to abs value of influence coef) for a particular frequency (i.e., SPL level) that can be used in future balancing cases to provide an initial guess for the trial weight.
14. A polar plot of the first trial will give a strong indication of where to place the second weight.
15. After the placement of the second trial weight and obtaining a polar plot of the results, the placement of the third weight may be of sufficient accuracy for final balancing. This reduces the balancing to an initial reading and three runs.
16. The polar plot method may be used to supplement the conventional influence coefficient method.

Three Trial Weight Method

The theory of the three trial weight method is well established. Nicholas, Gunter, and Allaire established that the method is highly suitable for balancing flexible bowed rotors with high amplification factors. The method proved to be more accurate than the influence coefficient method of balancing. Several ***MATLAB*** programs were written to perform the polar plots.

By applying the polar plotting of the trials after each run, information is obtained as to the best locations to apply the next trial. This is superior to arbitrarily placing weights around the wheel. By placing the weights near the proper balancing location, the nonlinearities are minimized.

Figure 24 represents the original vibration data taken for the three- run method . In the original data collection, the weights were moved around in an arbitrary manor. Figure 25 represents the plot of the three trials by graphical methods and the calculated balance. The rotor was run through the critical speed and the amplitude response plotted. The values used for the polar plot are the peak values and not selected at a constant speed.

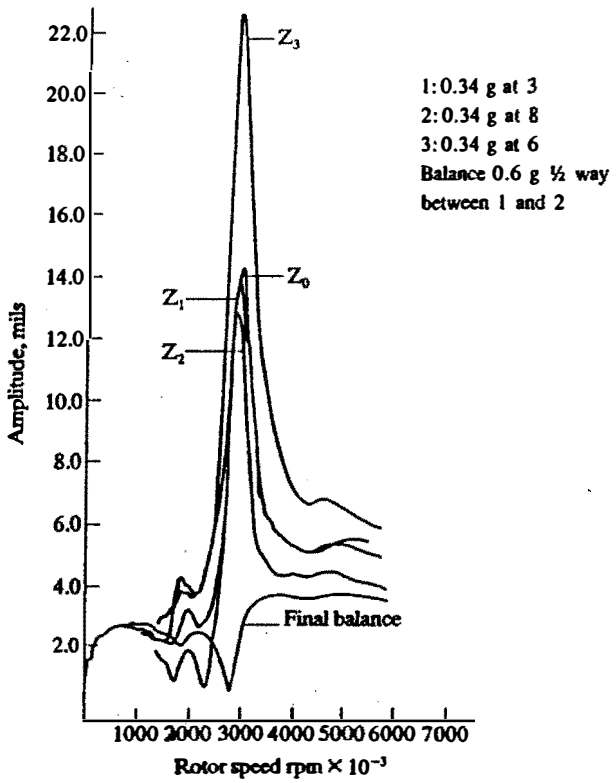

Figure 24 Initial Three Trial Weight Balancing Data For Bowed Rotor

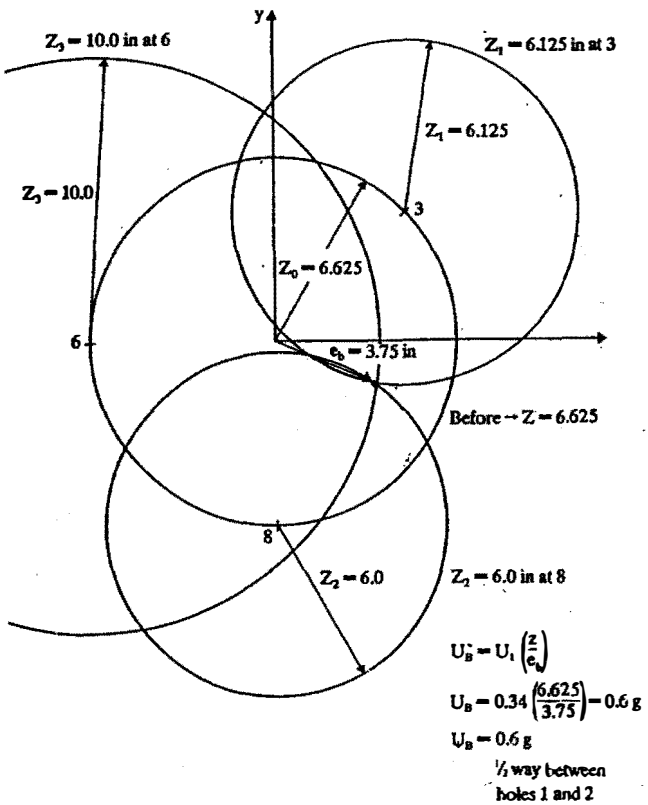

Figure 25 Graphical Balancing Solution (Nicholas, Gunter & Allaire 1976)

Fig 26 represents the MATLAB graphical plot of only the first two trial weights. After the 2 runs are made, there are two balance solutions. The point of the third run is to determine the correct solution. In this case, the correct balance can be computed from only the two runs. Since the circles are tangent, the proper balance weight and location may now be correctly predicted without a third run.

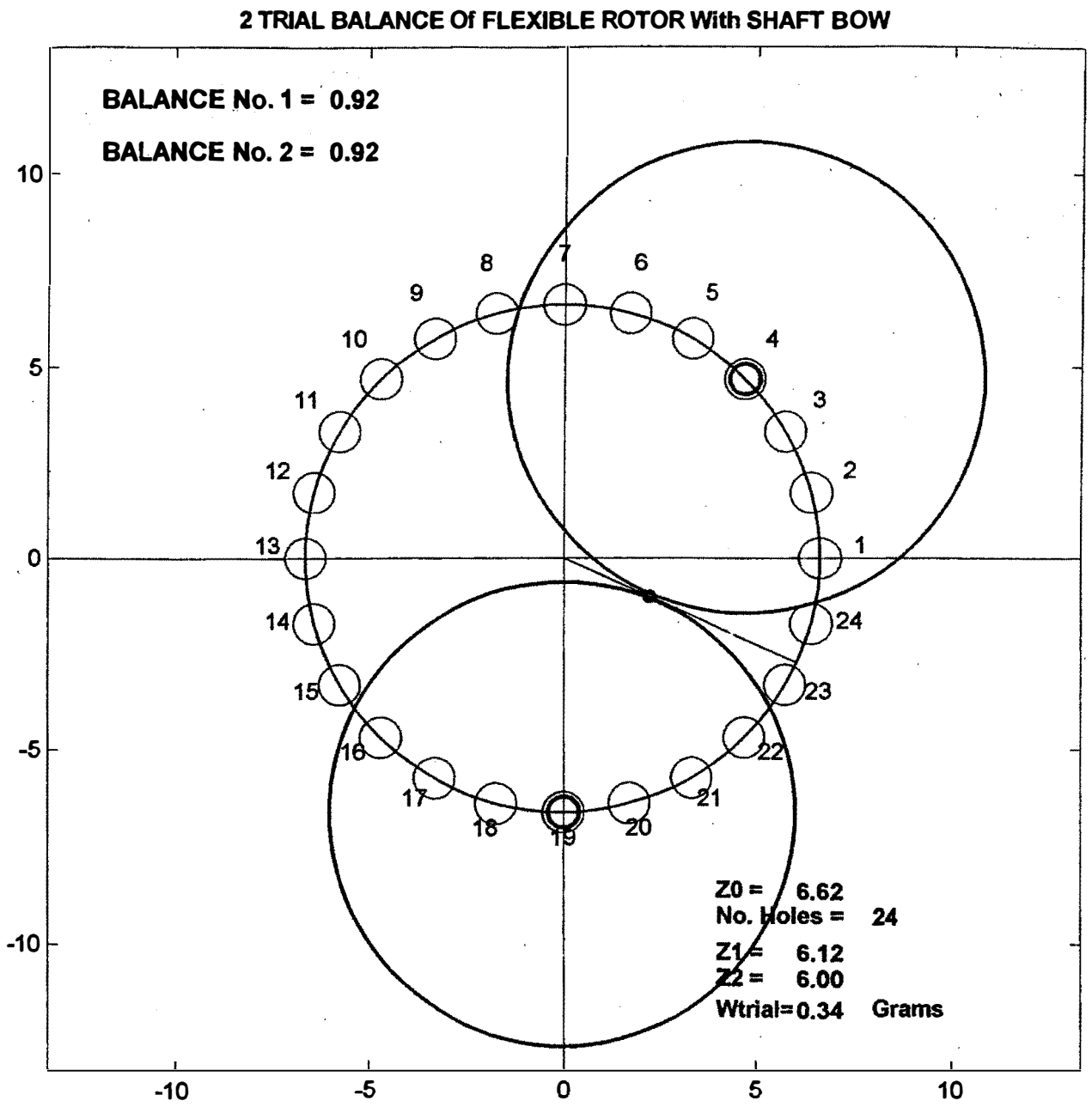

Figure 26 Balancing of Flexible Rotor With 2 Trial Runs

Fig 27 represents the MATLAB plot of the original graphics. The third trial weight was placed at location 13 as shown on the plot. Hole 13 is approximately 160 deg out of phase to the correct balance location. From the plots of the first two trial weights it is seen that either hole 23 or 24 should be used for the 3rd trial weight location. When one is over 120 deg from the correct or optimum balance location then nonlinear effects appear.

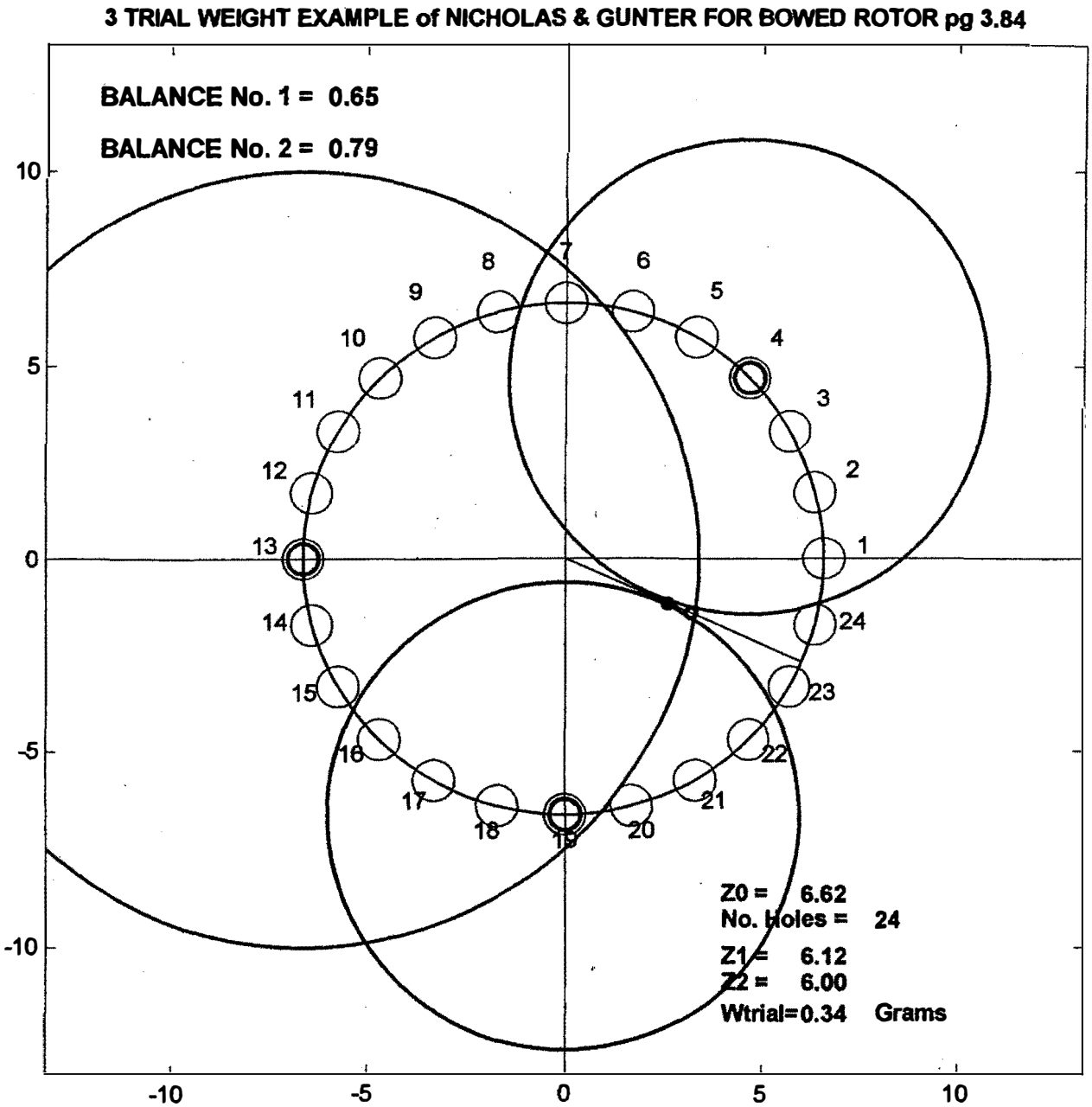

Figure 27 Balancing of Flexible Rotor With 3 Trial Runs

4.3 Representative Sound Pressure Levels (SPL) For Several Engines

SPL Levels For Various Engines

One of the objectives of the test cell balancing is to produce a smooth operating engine that generates a minimum of cabin noise when installed on the aircraft. It appears that the cabins of typical aircraft have tones in the vicinity of 100 Hz that are excited by the LP rotor engine unbalance. It appears that there are several engine modes that may couple with the aircraft structural modes to produce unwanted tones. It should be noted that all the engine-casing modes are not of the same importance in generating cabin tones. It appears that engine modes in the vicinity of 90 to 115 Hz have the most influence.

Figure 28 represents the SPL on Engine 112 on the left side of Airplane 52. This vibration shows a peak near 6,900 CPM (115 Hz). The SPL was effectively eliminated by a fan balance correction of 9.1 grams at 0 deg. Above 7,400 CPM (123 Hz), the SPL level reduces rapidly. Therefore, for the cases in which a distinct peak in SPL is observed, it is preferable to balance at the peak, rather then at the maximum speed.

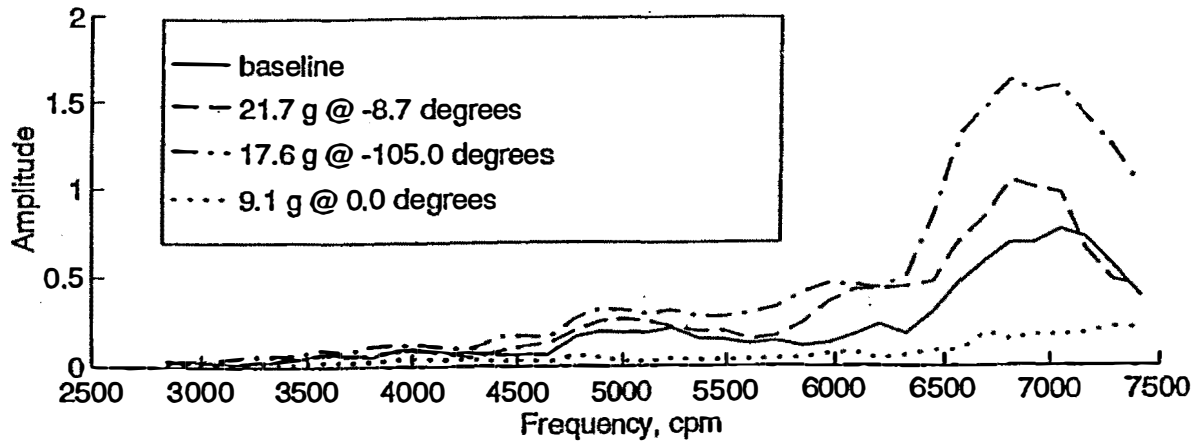

Figure 28 SPL Vibration on Engine 112-L

Two Trial Weight Balancing on SPL Level For Engine 116

Figure 29 represents the SPL on Engine 116 on the right side of Airplane 52. The SPL vibration appears to have a sharper amplification factor than Engine 112. The major frequency is at 115 Hz. There are also minor modes excited at 5,600 CPM (94 Hz) and at 4,200 CPM (70 Hz). The SPL resonance mode at 6,800 RPM appears to have a higher amplification factor then does Engine 112-L. Note that in this balancing case two of the trial weights are identical. Figure 30 represents the 2 trial weight balance calculation for Engine 116-R on Airplane 52. The intersection of the second trial with the first trial of Figure 30 indicates two solutions. The first balance solution is 5.2 grams at hole 11. The second balance solution is 3.3 grams between holes 11 & 12. This is not likely. Thus, the movement of the balance weight from hole 11 to hole 10 should cause an even greater improvement in the SPL level. Note that the two or three trial weight method does not contradict the influence coefficient method, but supplements it and provides confirmation.

Figure 29 SPL Vibration on Engine 116-R , Airplane 52

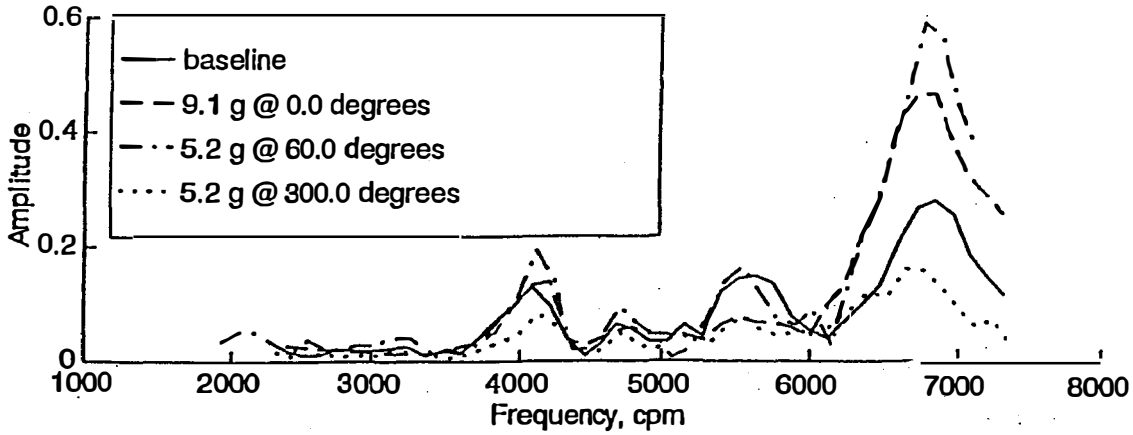

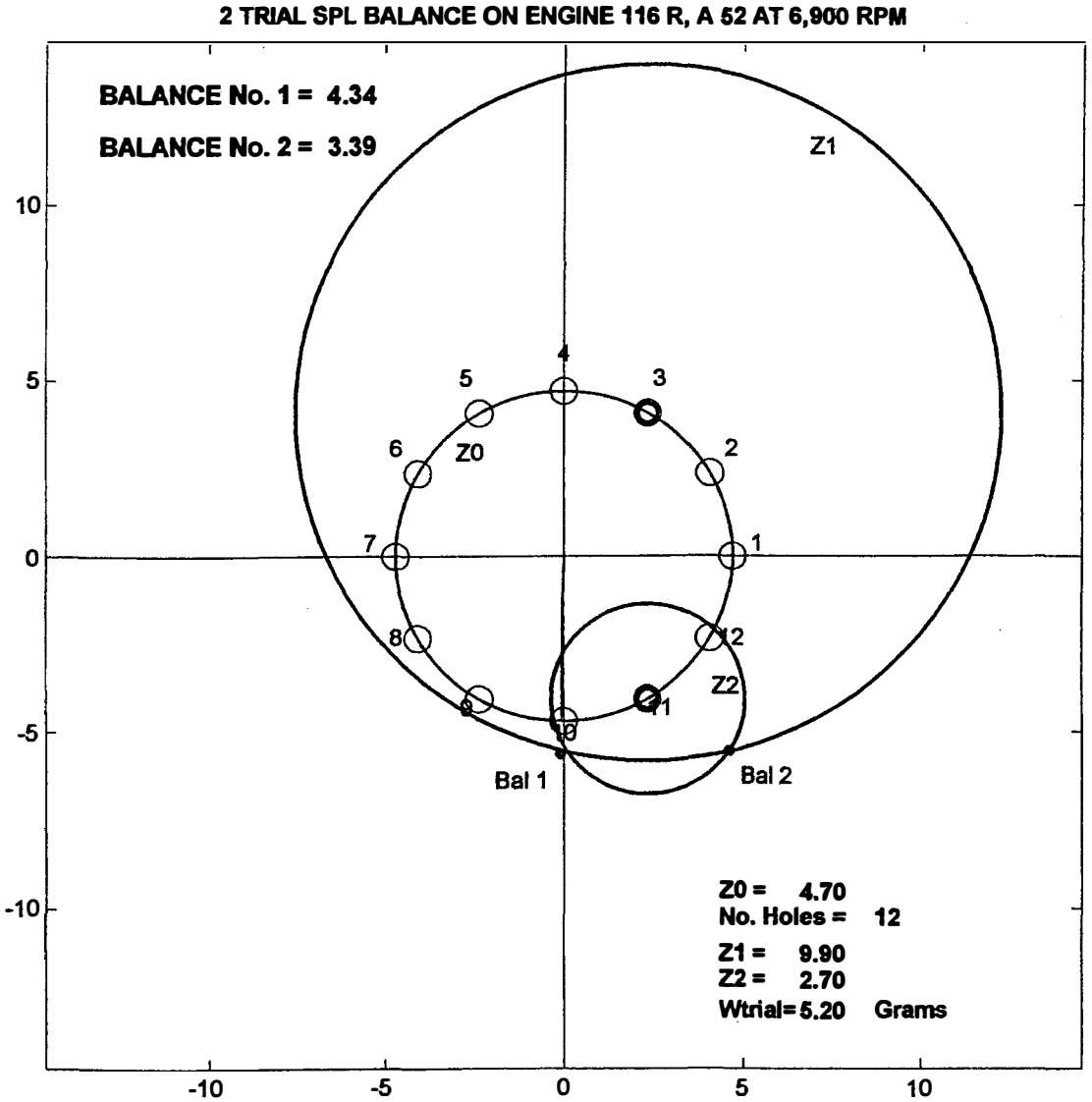

Figure 30 2 Trial Weight Balancing on Engine 116-R , Airplane 52

4.4 Two-Trial Balancing Using Engine Response

Balancing Using VFFV

The two- or three-trial balancing procedure may also be applied to engine data. Figure 31, for example, represents the front frame vertical motion (VFFV) taken during the engine testing. There were two of the three runs made with 8.8 grams at 60 deg and 240 deg. The first 8.8-gram weight is shown at location No. 3. The amplitude is larger than the base circle of 0.71 in/sec. The first trial, Z1, intersects the base circle, Z0, at holes 7 and 11, as shown in Figure 32.

The next trial weight should be between holes 7 through 11. The other holes should be excluded, as these trial locations would result in a larger response than the initial base amplitude. The second trial was at location 9 and represents an excellent balance run. Possible balance corrections could be 10.6 grams at hole 8, or 10.6 grams at hole 10. A third balance run to complete the three-trial-run method would be to move the 8.8-gram balance weight to hole No. 8.

Balancing Using FFV From Engine 109-R, Airplane 47

Figure 33 represents the front frame vertical (FFV) vibration on Engine 109-R with 9.1 grams placed at 150 deg and 210 deg. The final move to 210 deg has reduced the amplitude in half. From an observation of the data without phase, it is not apparent what the next correction should be. Figure 34 shows a polar plot of the two trials. The first trial, plotted at location 11, intersects the base circles at holes 8 and 14. The placement of the weight at hole 15 represents a good shot.

From the intersection oft he plots for Z1 and Z2, two balancing solutions are obtained. These solutions are 7.5 or 16.6 gras between holes 13 and 14. However, from previous balancing runs, it is known that the 16.6-gram balancing solution is too large. Therefore, the correct balancing solution is 7.5 grams, split between holes 13 and 14. This is not practical to do in the field, since the selection of weights available is limited. A final balance move would be to move the weight from hole 15 to hole 14. This balance example illustrates the importance of having a sufficient number of balancing holes on the fan for final balance correction. The current fan rotor has only 12 balancing holes.

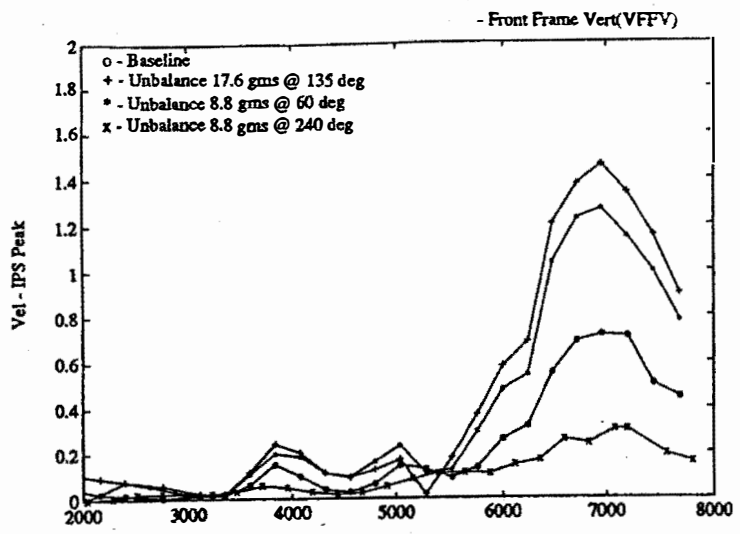

Figure 31 - Front Frame Vertical (VFFV)

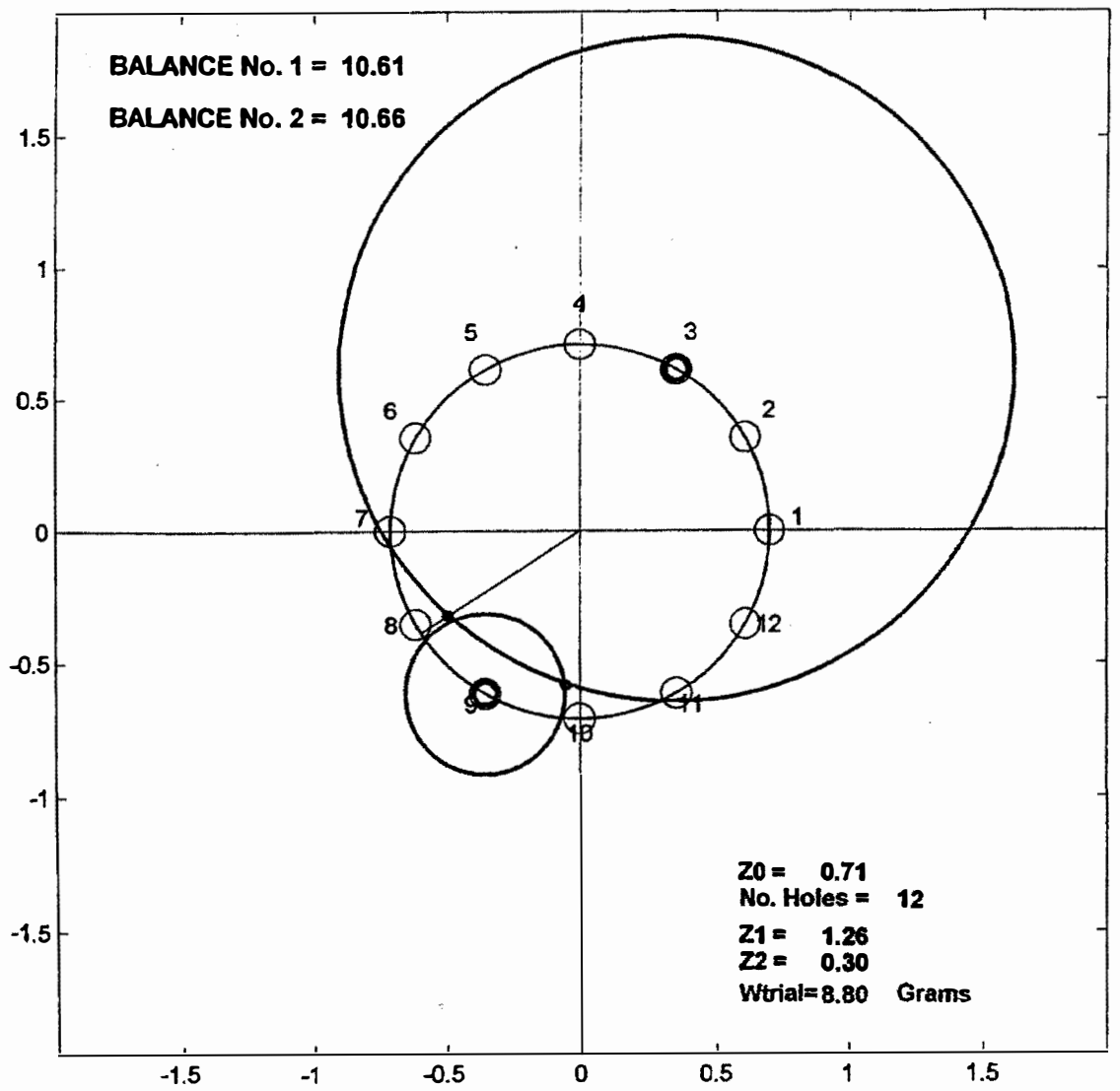

Figure 32 2 Trial Weight Balancing Using VFFV

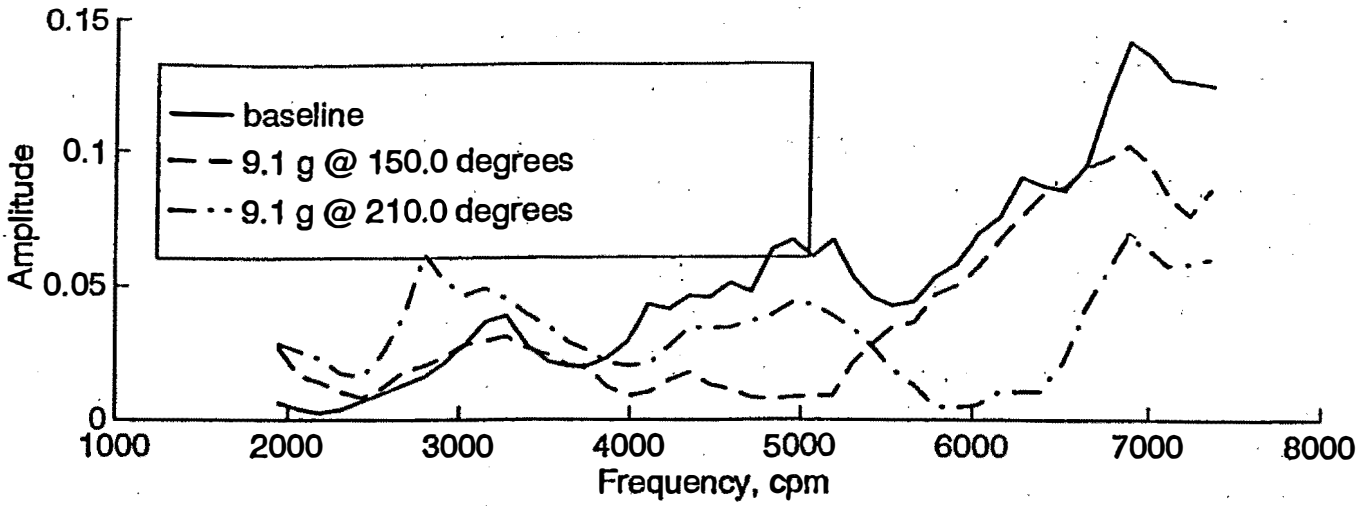

Figure 33 Front Frame Vertical (FFV) Vibration on Engine 109-R, Airplane 47

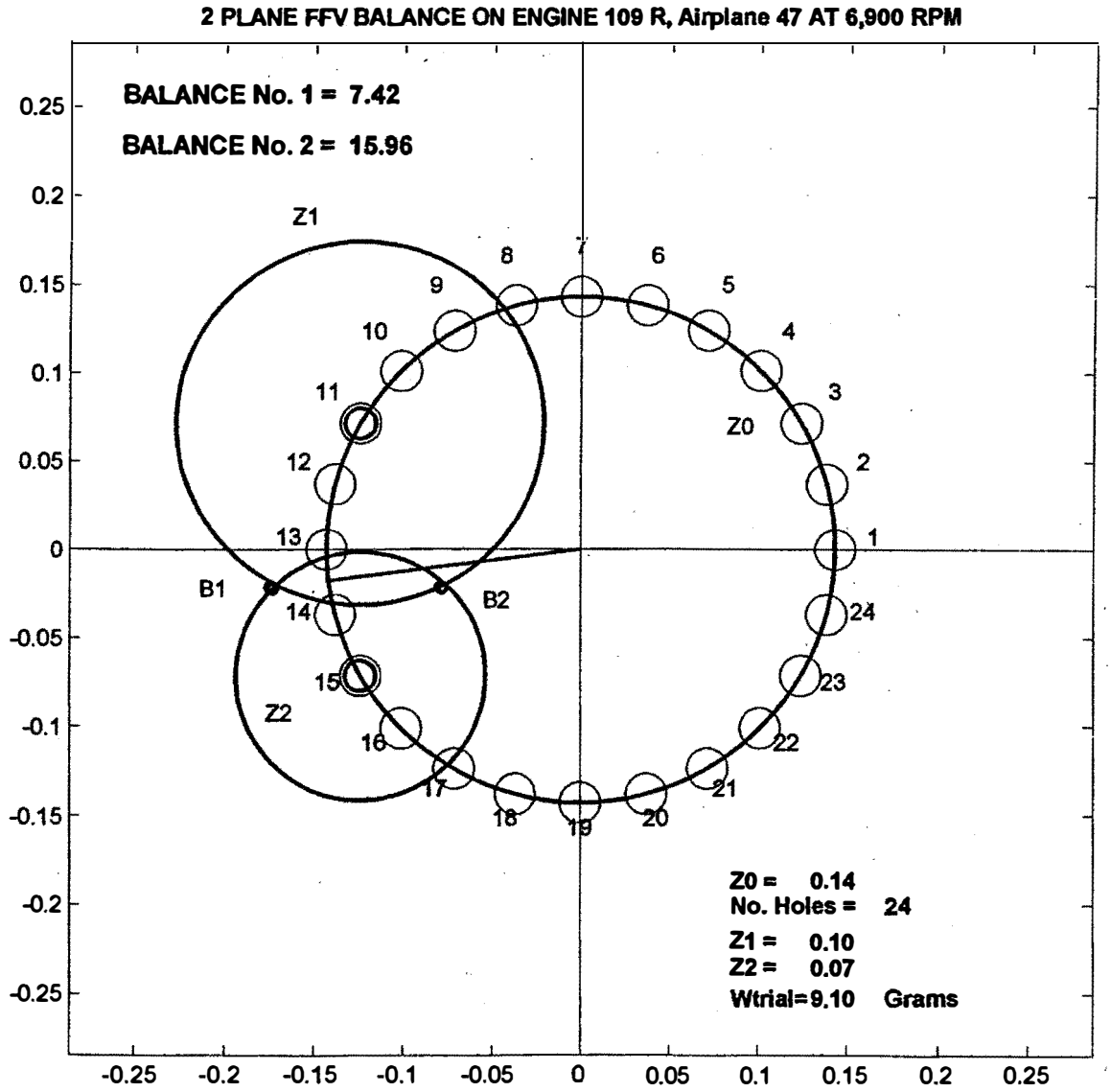

Figure 34 2 Trial Weight Balancing Using FFV on Engine 109R, Airplane 47